

Aspects and Applications of THz FELs

A.F.G. van der Meer

FELIX Laboratory

Radboud university, Nijmegen

Outline

Aspects of THz - FELs:

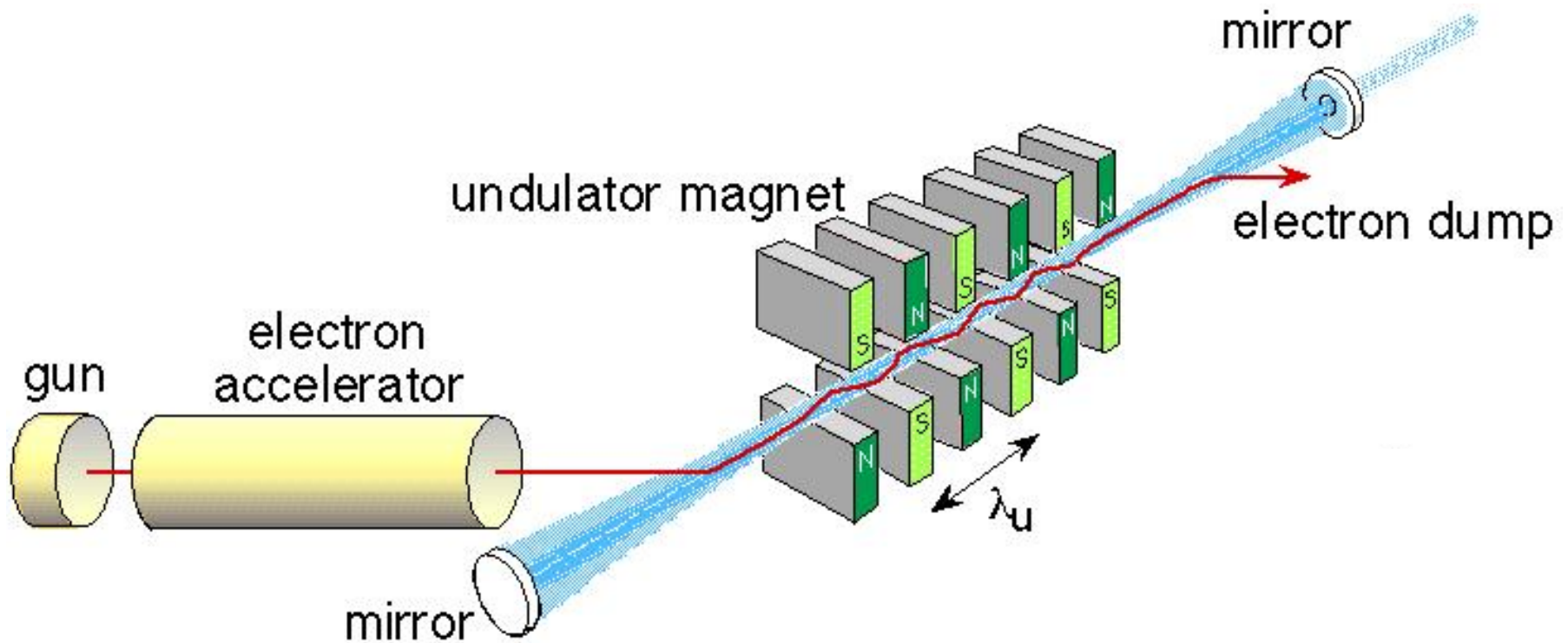
- Radiation bandwidth
- Resonator issues
- Slippage effects

Applications:

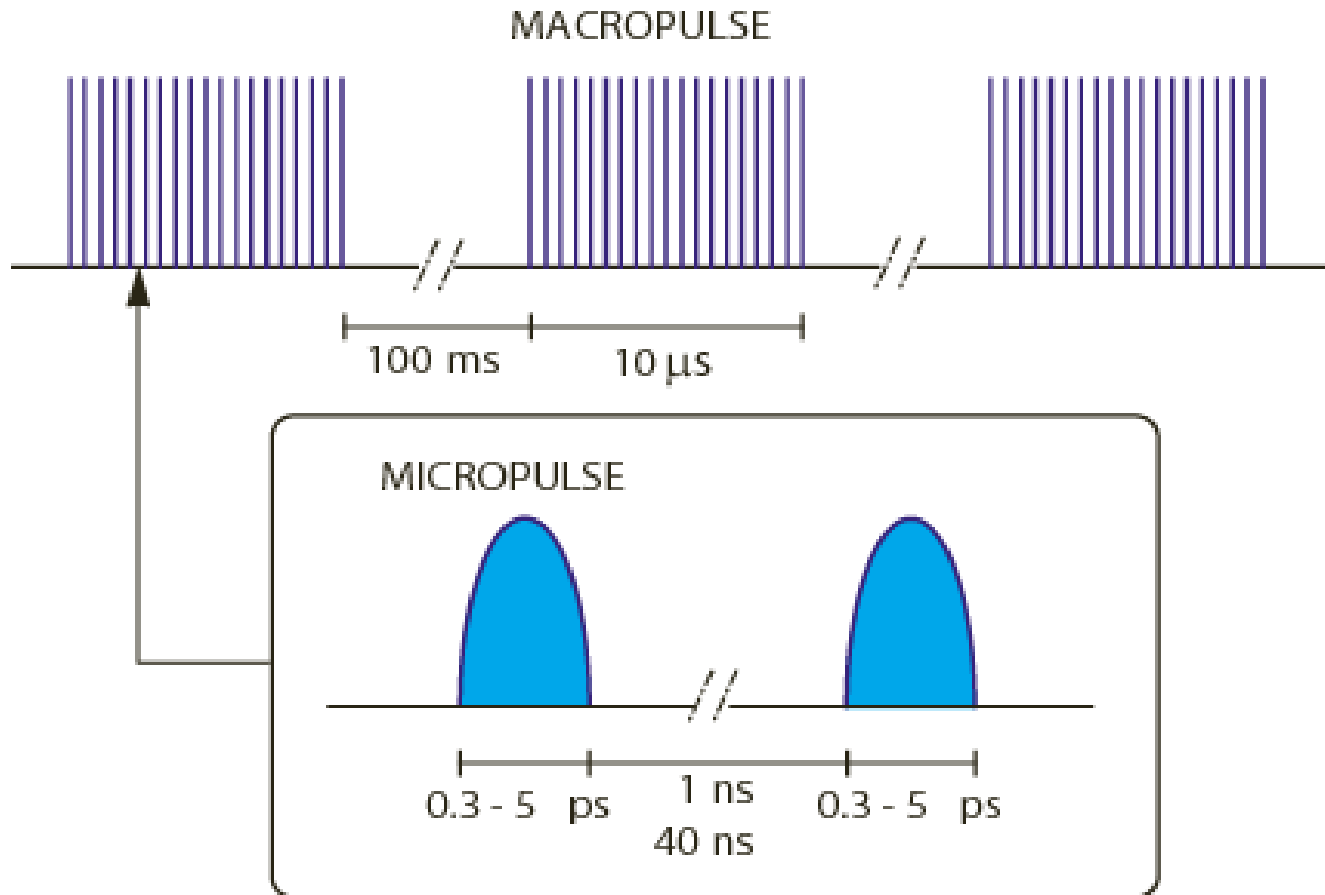
- nonlinear optics
- nano-spectroscopy
- 'action spectroscopy'

The FELIX laboratory

Generic layout

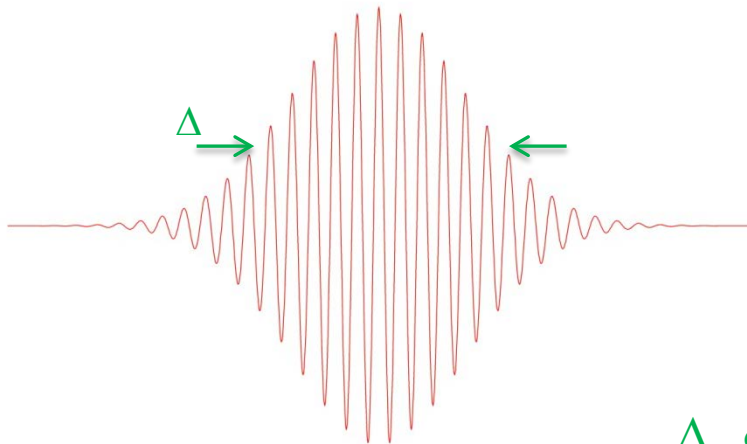


Radiation bandwidth: linac pulse structure

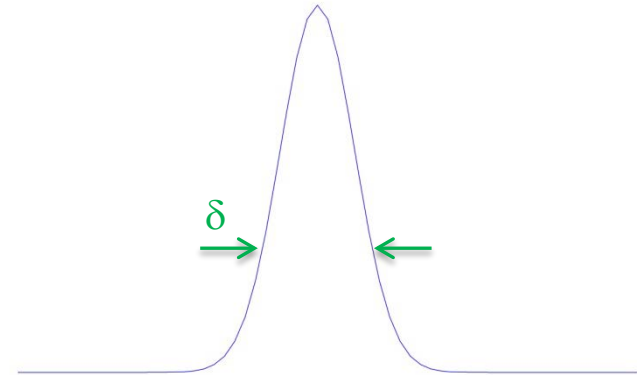


Radiation bandwidth: Fourier transform

pulse shape



spectrum

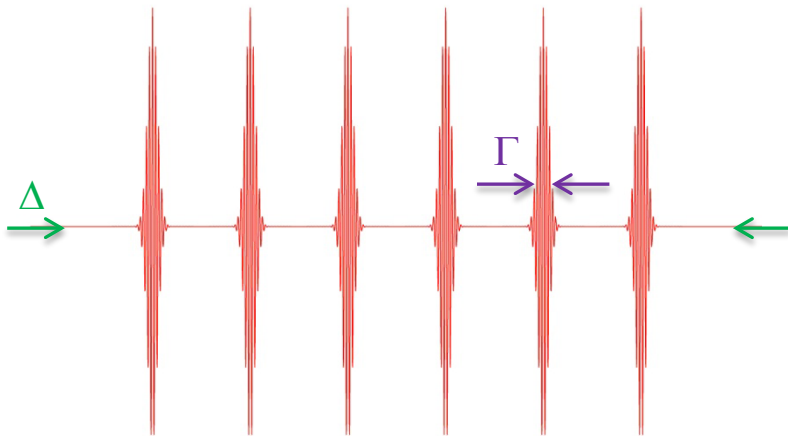


$$\Delta \cdot \delta \approx \text{constant}$$

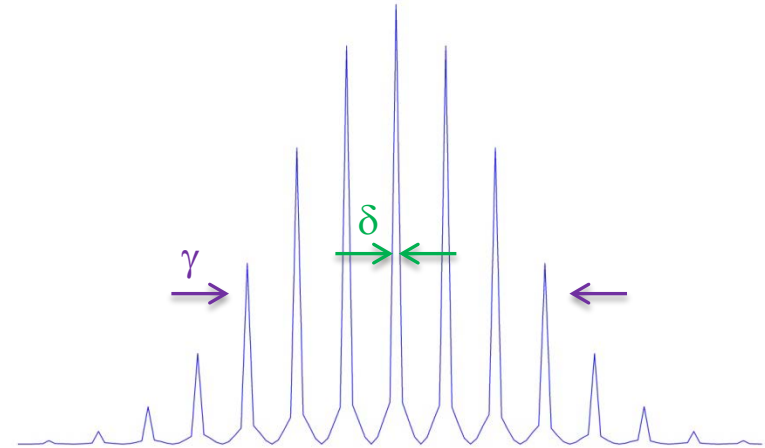
'transform limited' : no frequency / phase fluctuations of the carrier

Radiation bandwidth: Fourier transform

multiple pulses



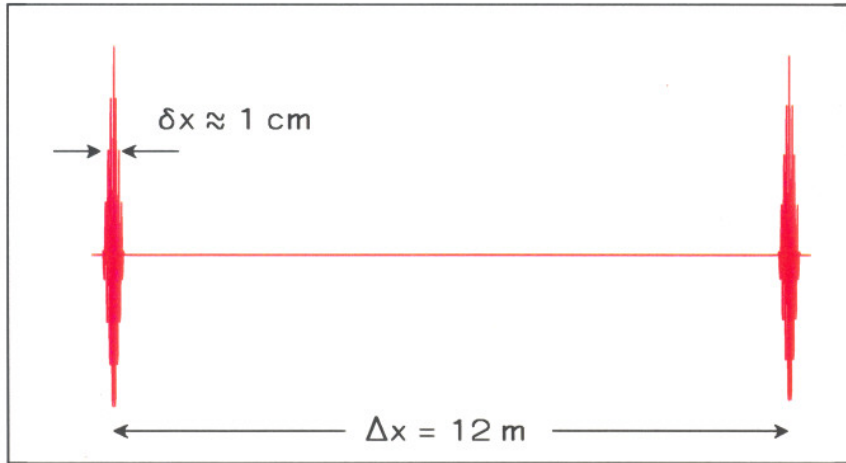
multiple spikes



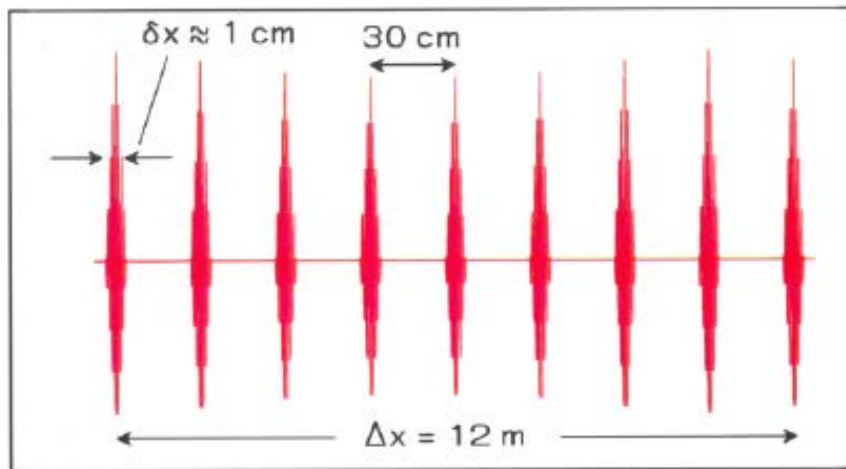
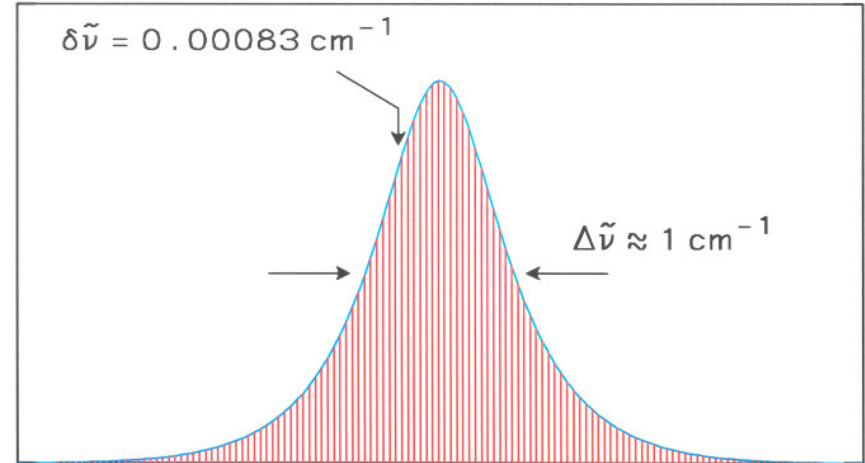
$$\Gamma \cdot \gamma = O(1)$$

$$\Delta \cdot \delta = O(1)$$

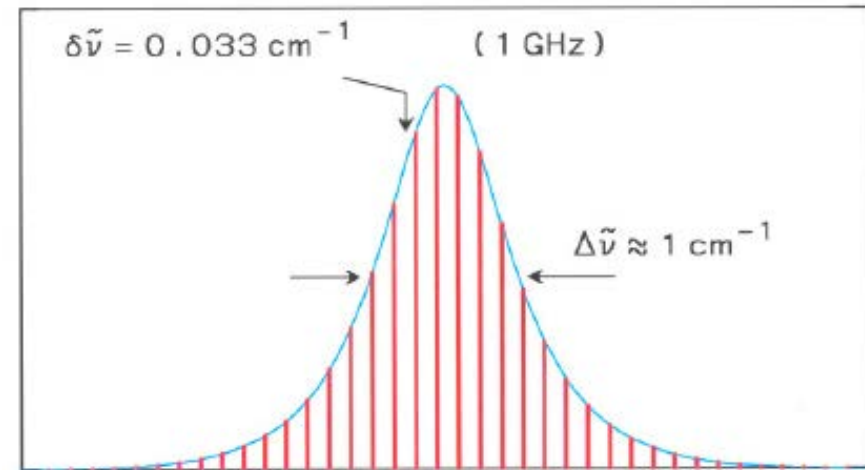
Radiation bandwidth: phase locking



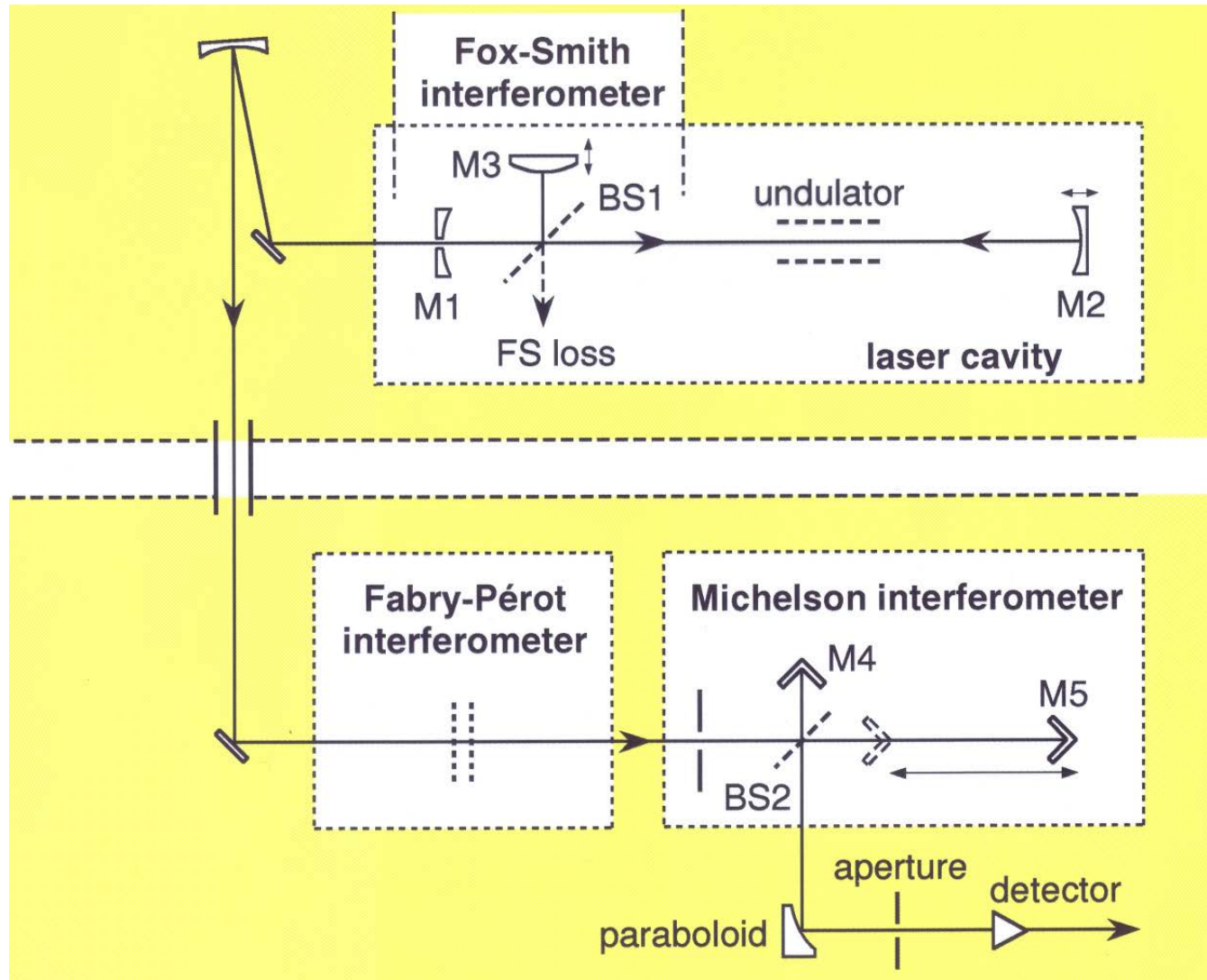
$M = 1000 - 2000$



$M = 25 - 50$

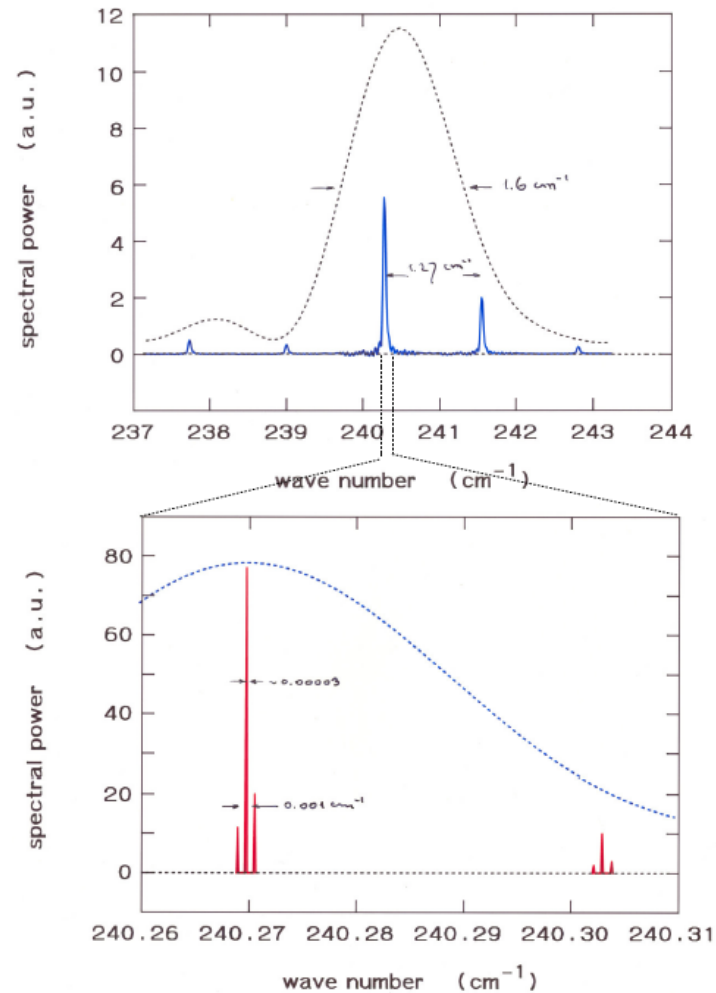


Phase locking & single mode selection



Phase locking & single mode selection

Experimental result

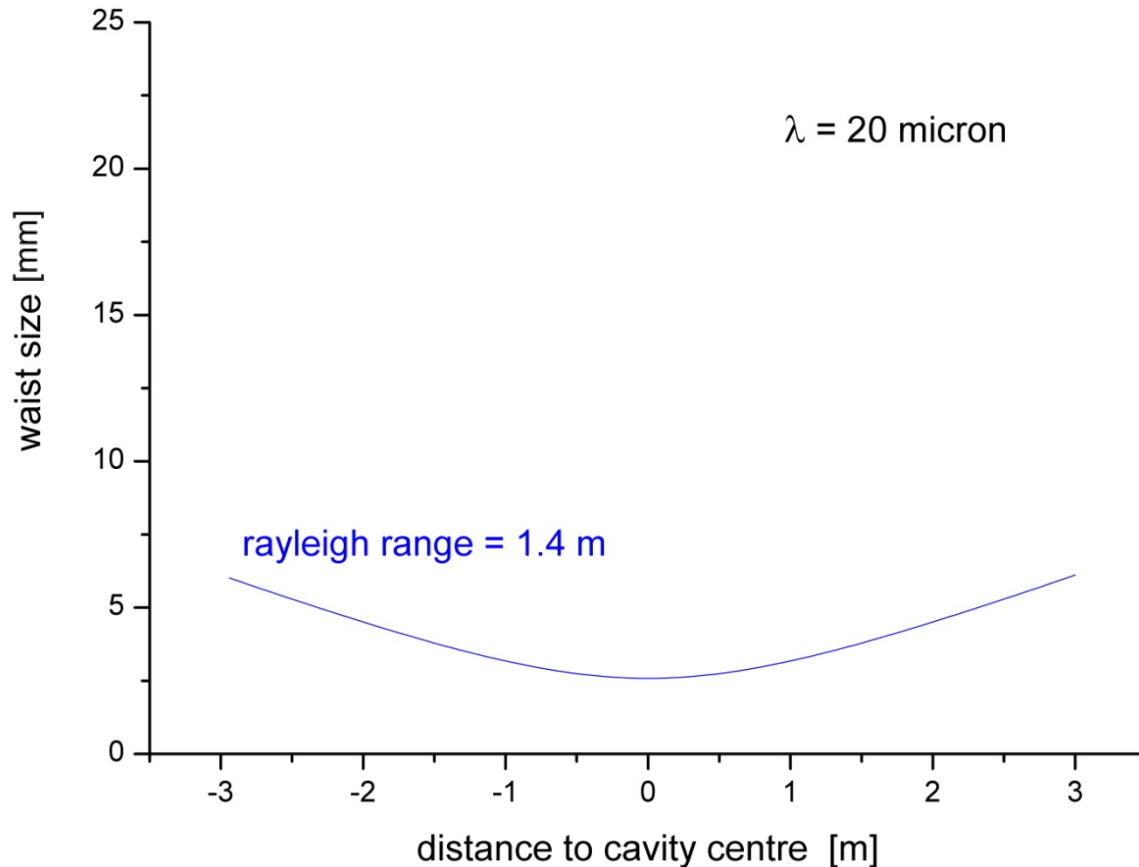


Resonator issues

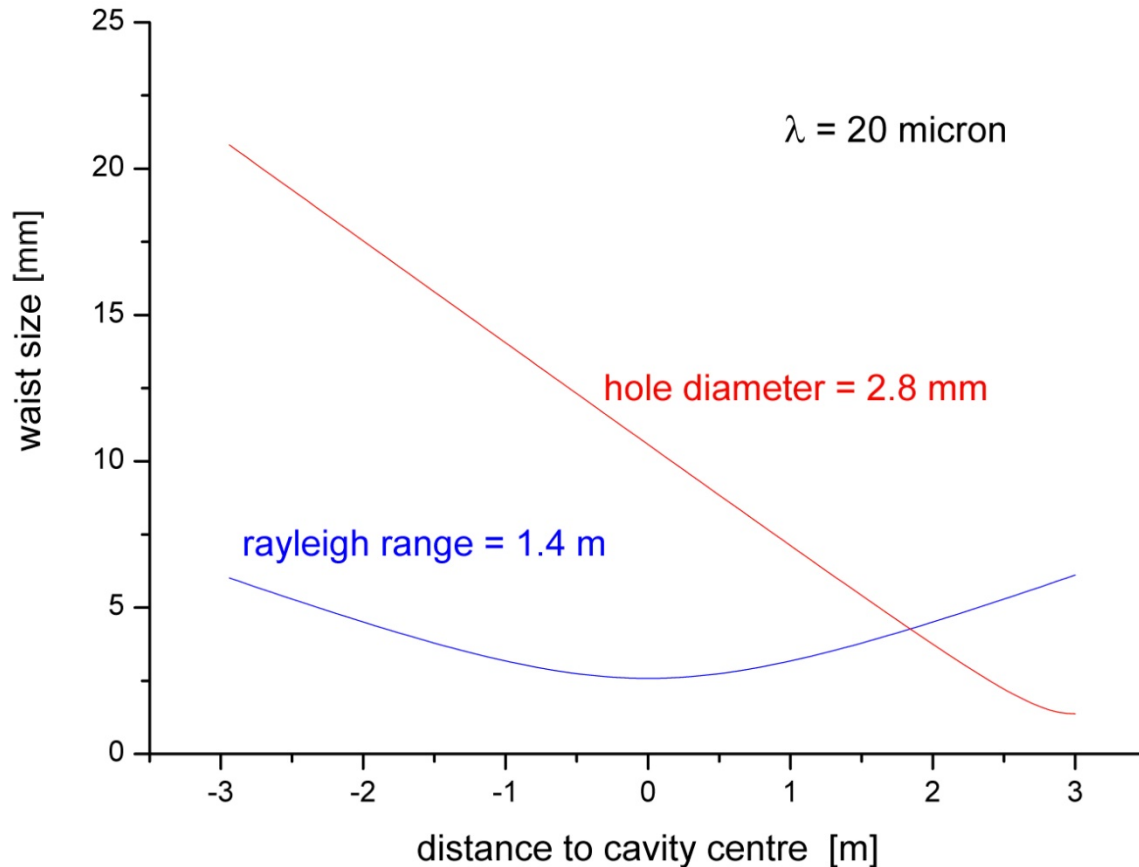
out-coupling schemes:

- 'semi-transparent' mirrors
- beam splitter
- hole coupling
- edge coupling

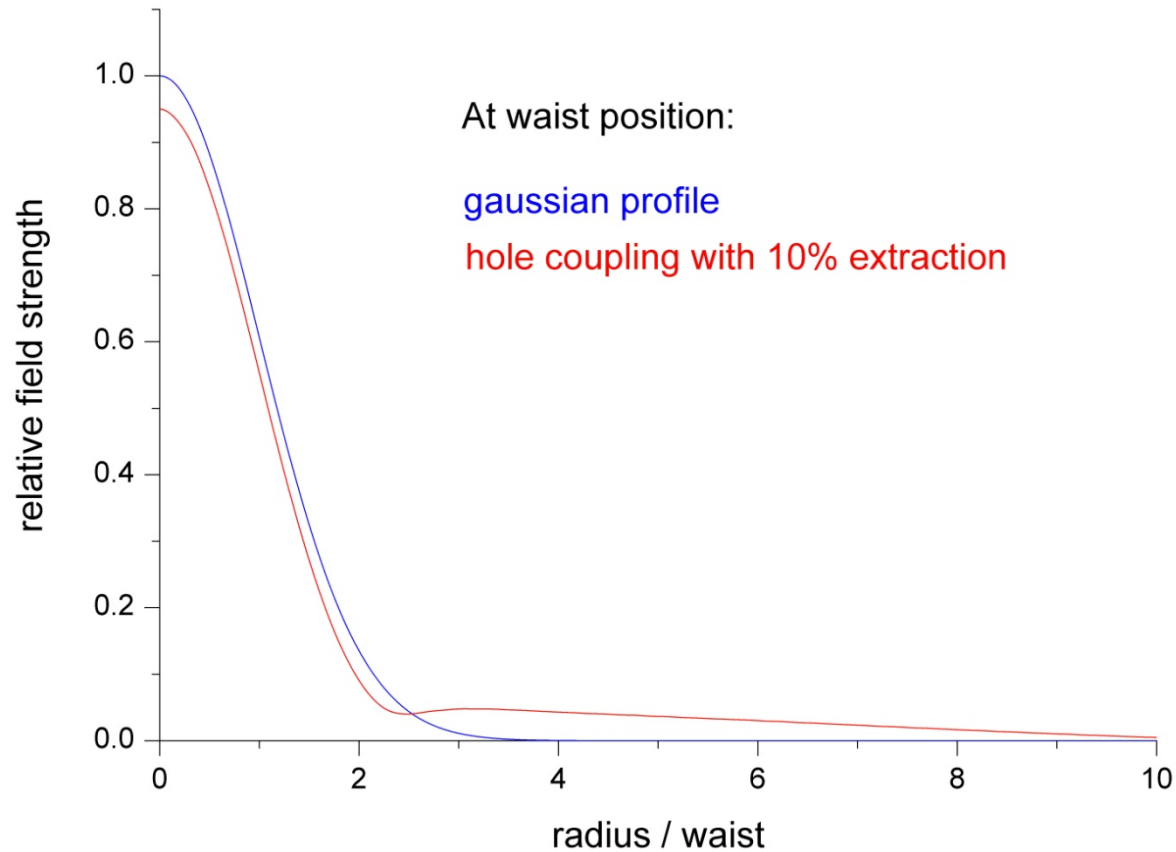
Resonator issues: on-axis hole coupling



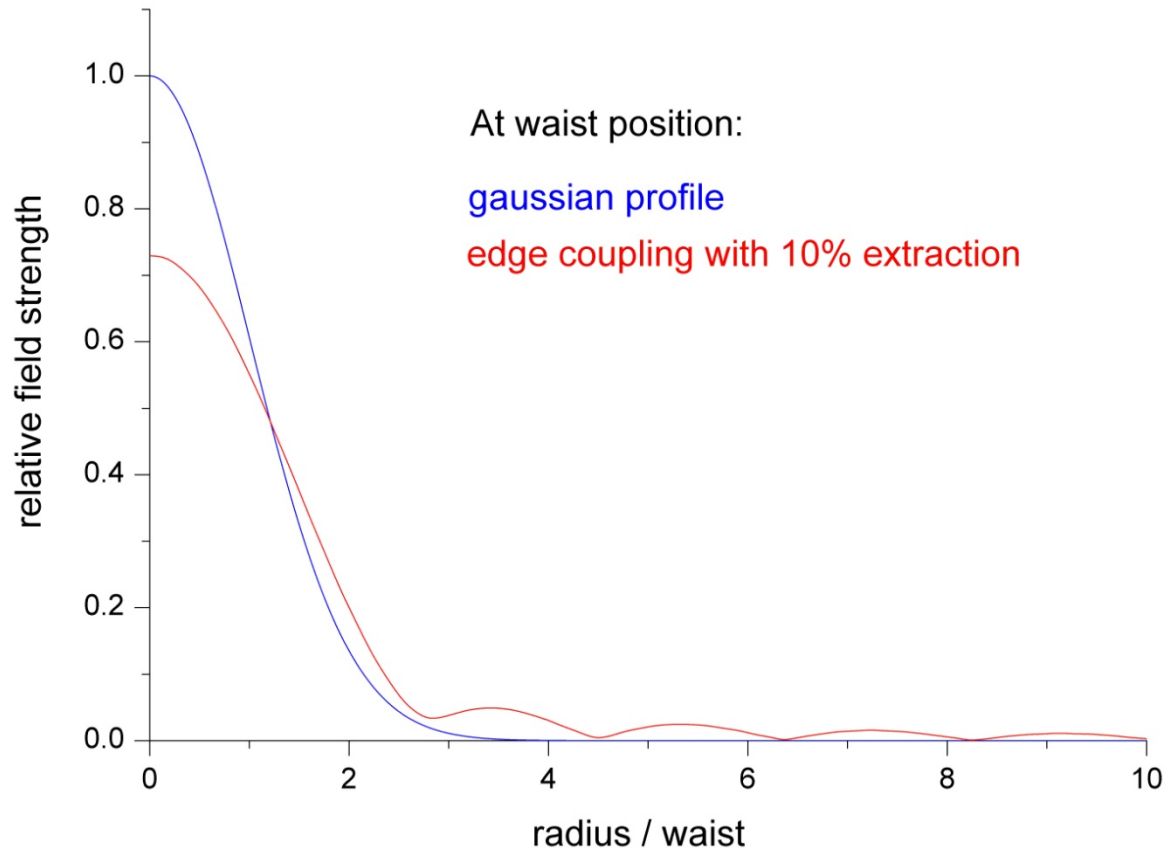
Resonator issues: on-axis hole coupling



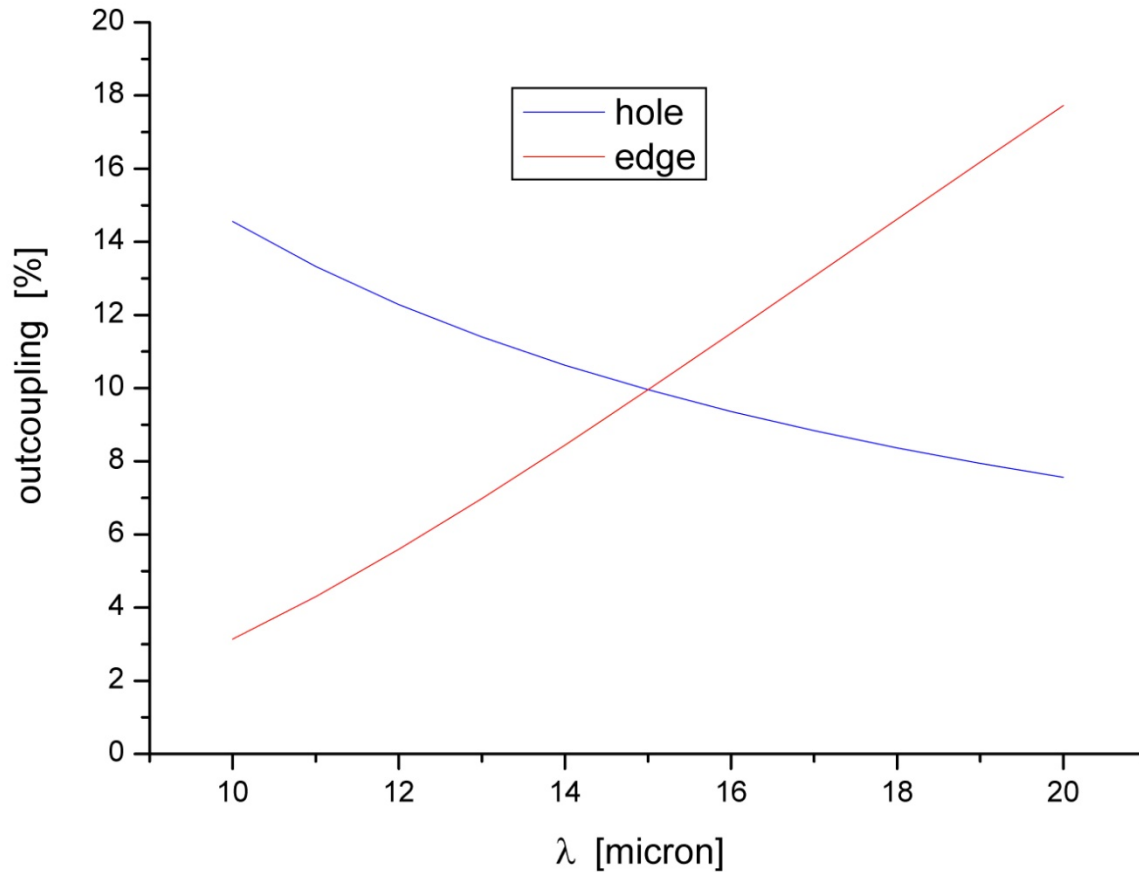
Resonator issues: on-axis hole coupling



Resonator issues: edge-coupling

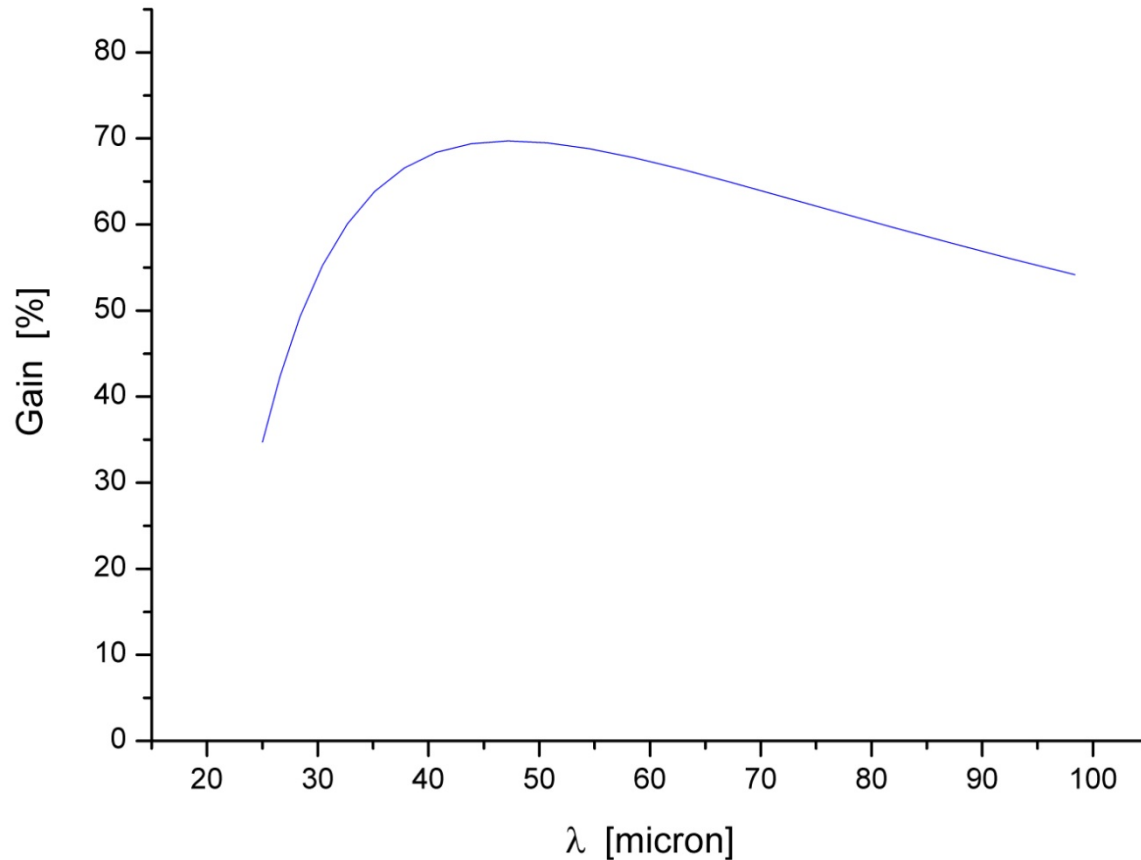


Hole vs edge coupling: λ - dependence

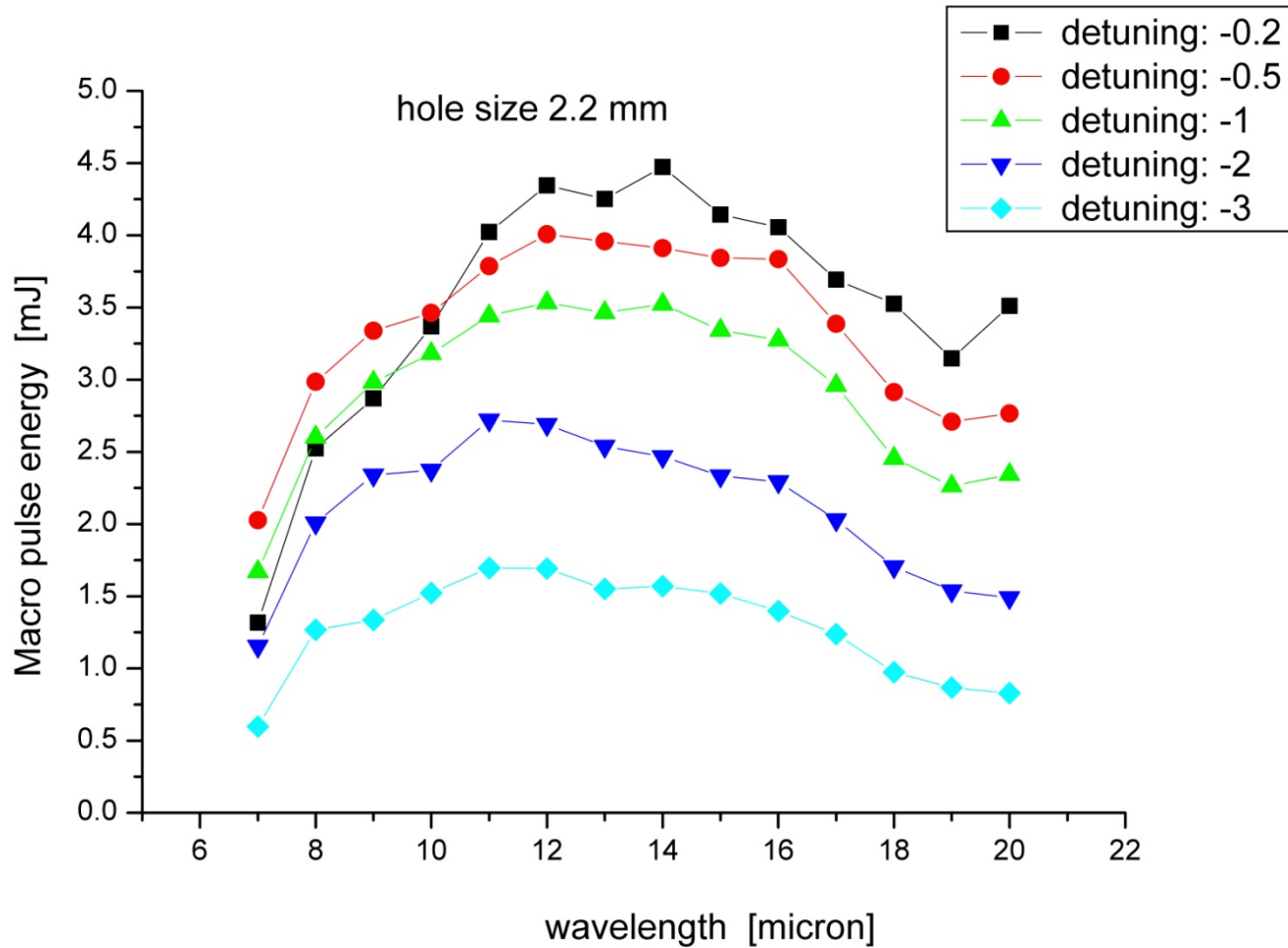


Hole vs edge coupling: λ - dependence

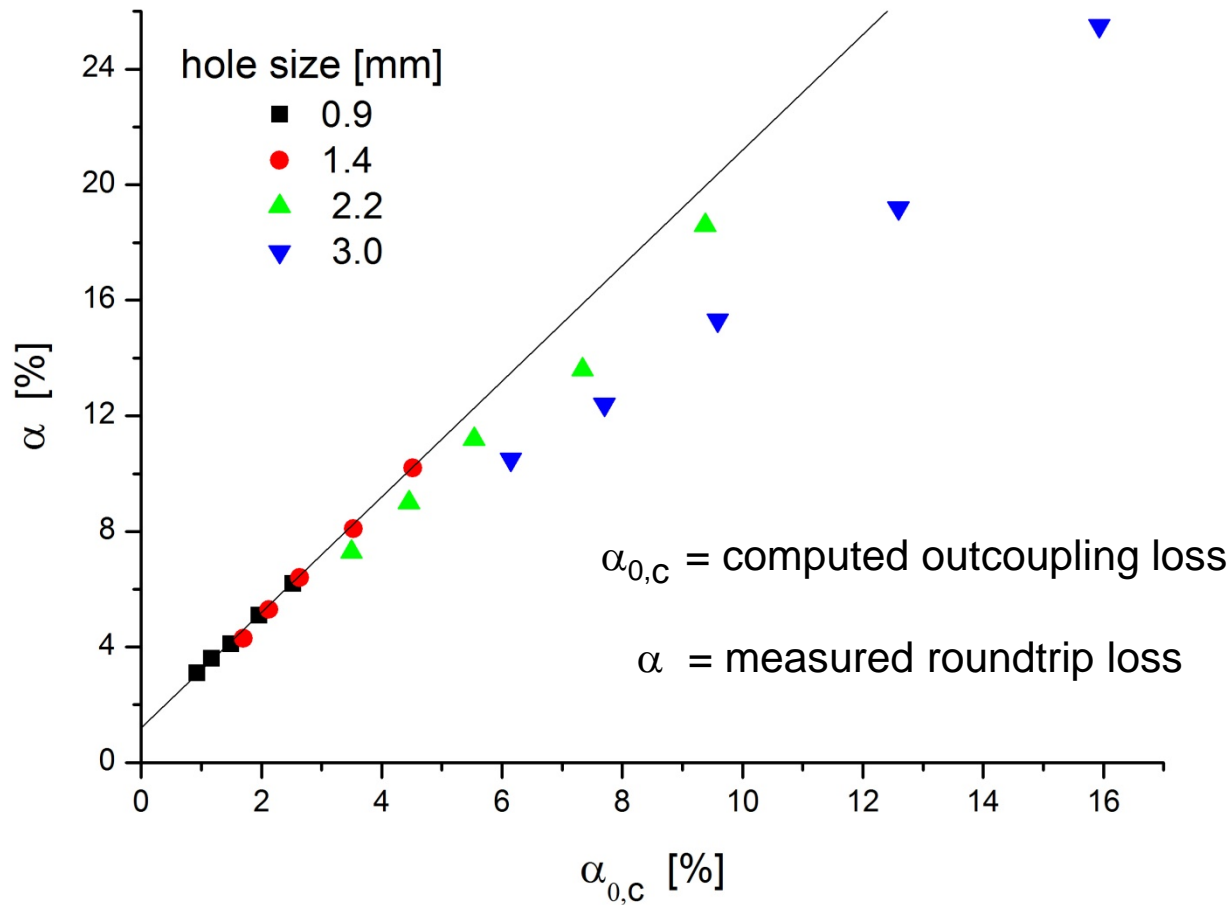
Typical gain curve



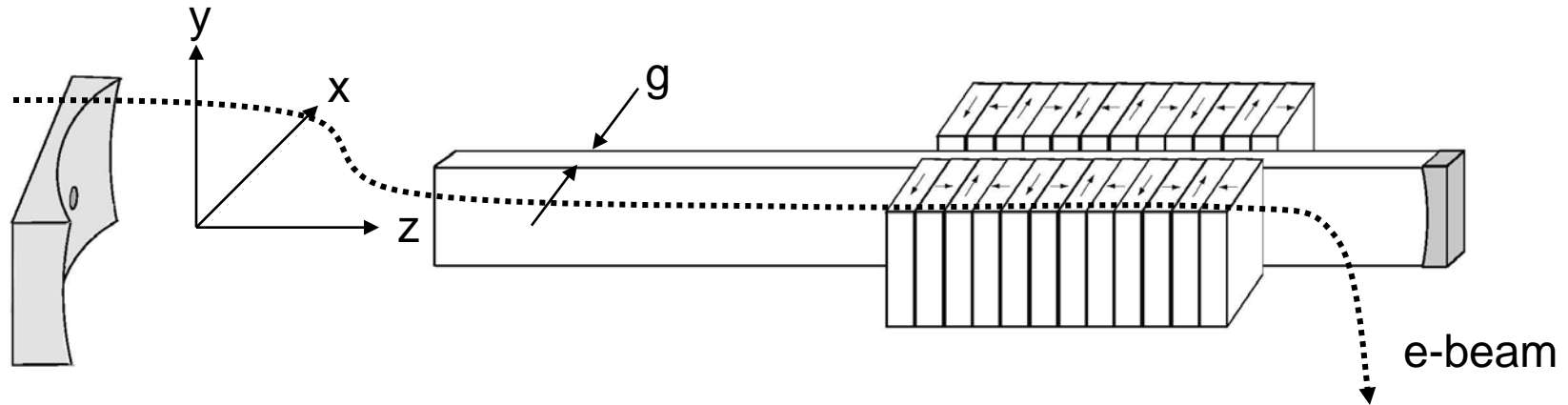
Hole coupling: tuning curves



Hole coupling: measured losses



Partial-waveguide resonator

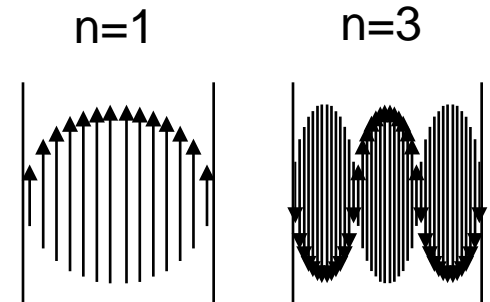


Eigenmodes are a combination of TE and Hermit-Gaussian modes:

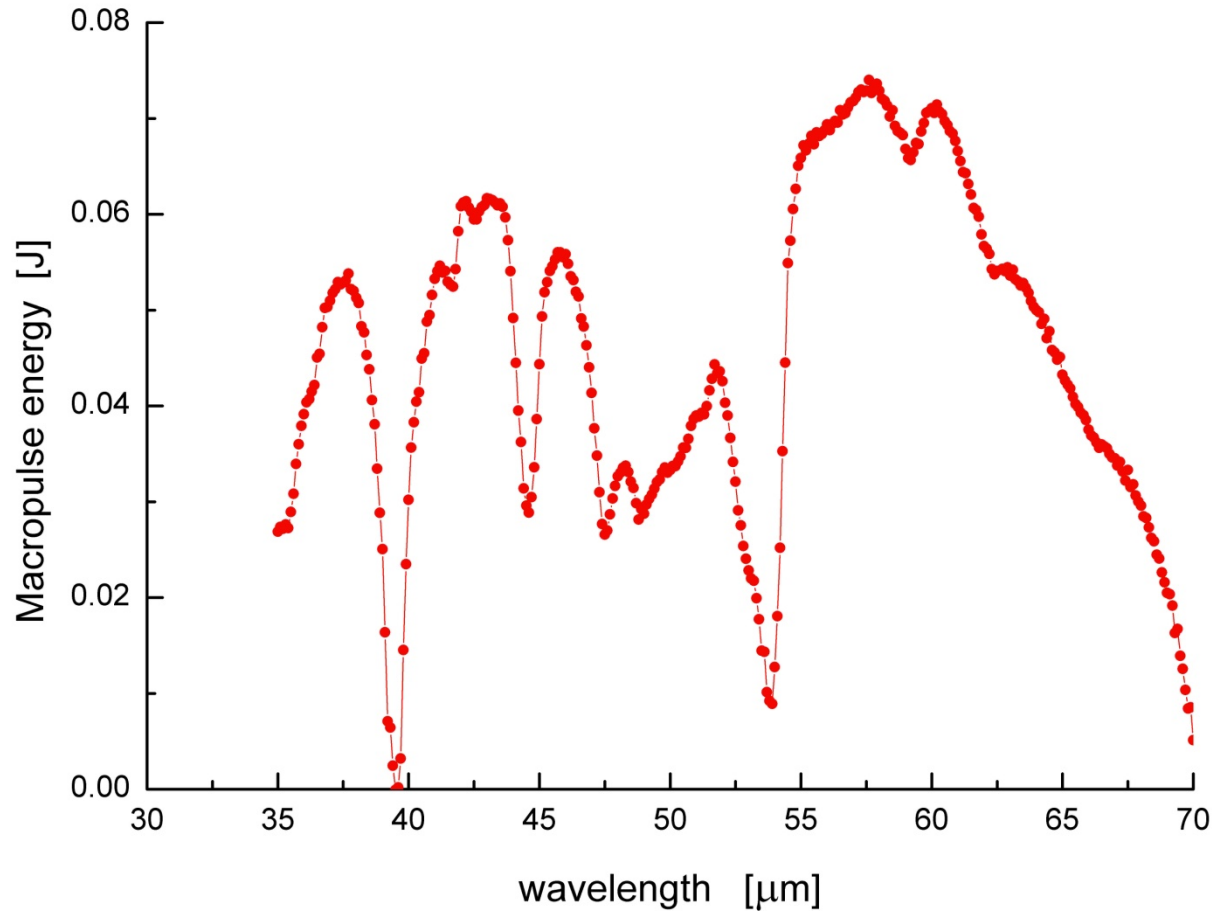
$$\Psi_{m,n}(x, y, z) \sim H_m\left(\frac{\sqrt{2}y}{w(z)}\right) \sin\left(\frac{nx\pi}{g}\right) \exp\left(\frac{-y^2}{w^2(z)} + i\left(\frac{k_n^z y^2}{2R(z)} - \left(m + \frac{1}{2}\right) \tan^{-1} \frac{z}{z_r}\right)\right)$$

$$\text{with } w(z) = w_0 \cdot \sqrt{1 + \frac{z^2}{z_r^2}}, \quad k_n^z = \sqrt{k^2 - n^2 k_\perp^2}, \quad R(z) = z + \frac{z_r^2}{z}$$

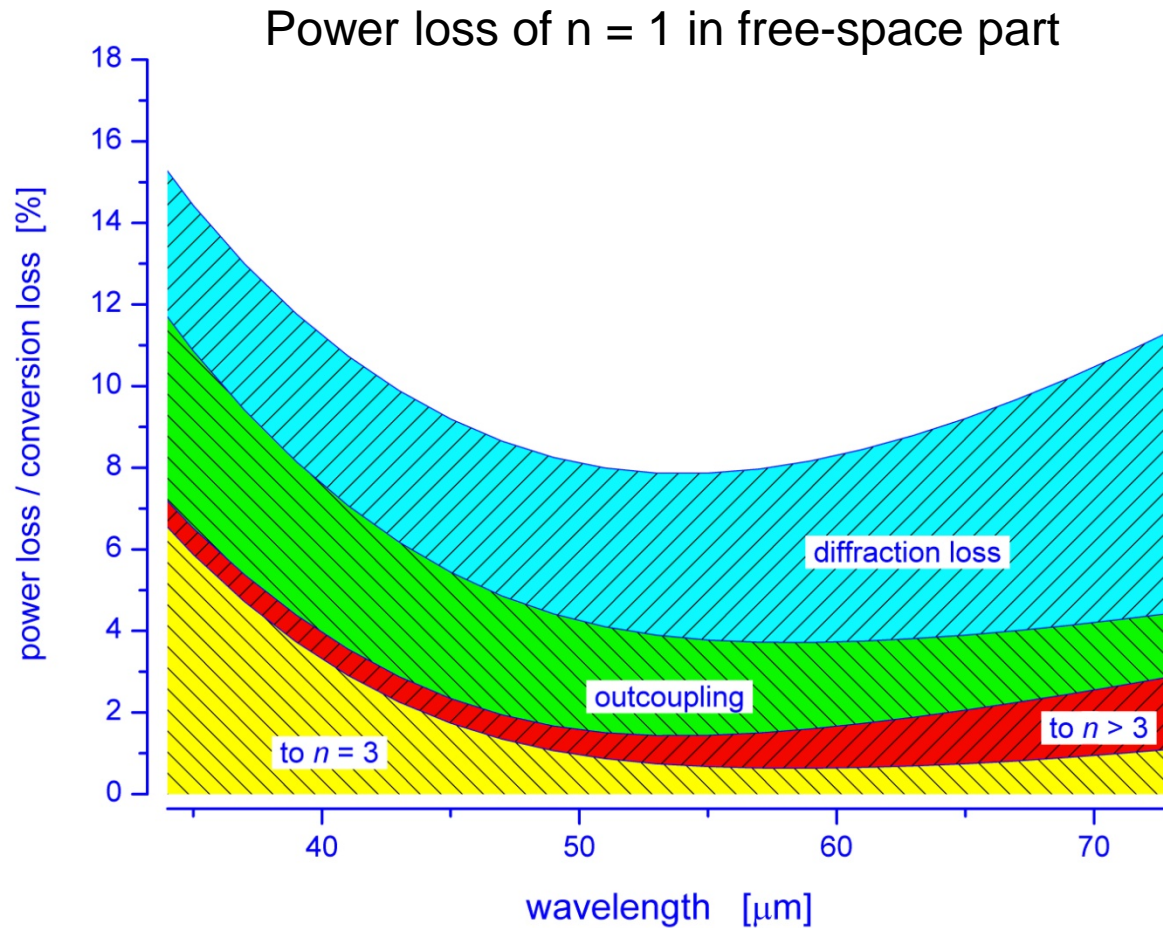
$$\text{and } k_\perp = \frac{\pi}{g}, \quad \text{where } k \text{ is the wave vector in vacuum, } z_r \text{ the Rayleigh range and } w_0 \text{ the waist}$$



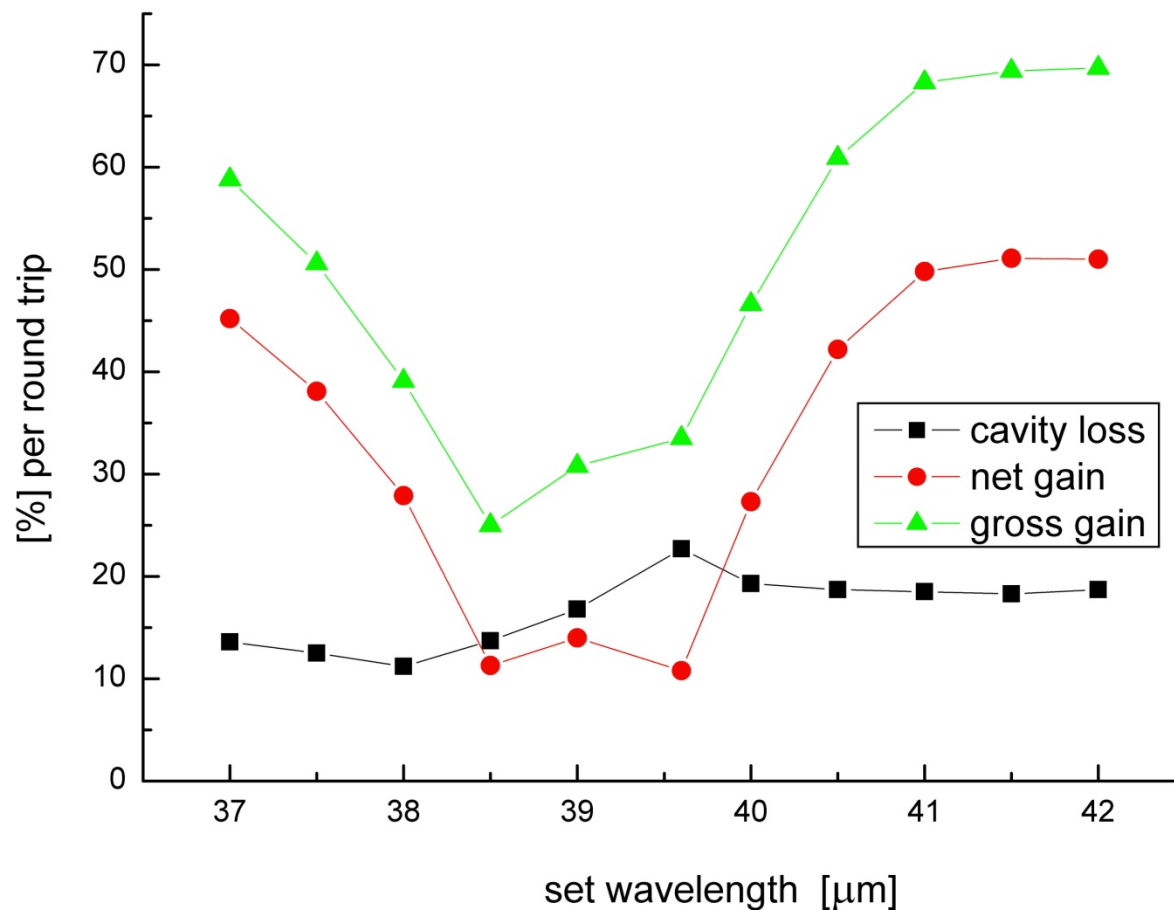
Typical tuning curve FELIX waveguide FEL



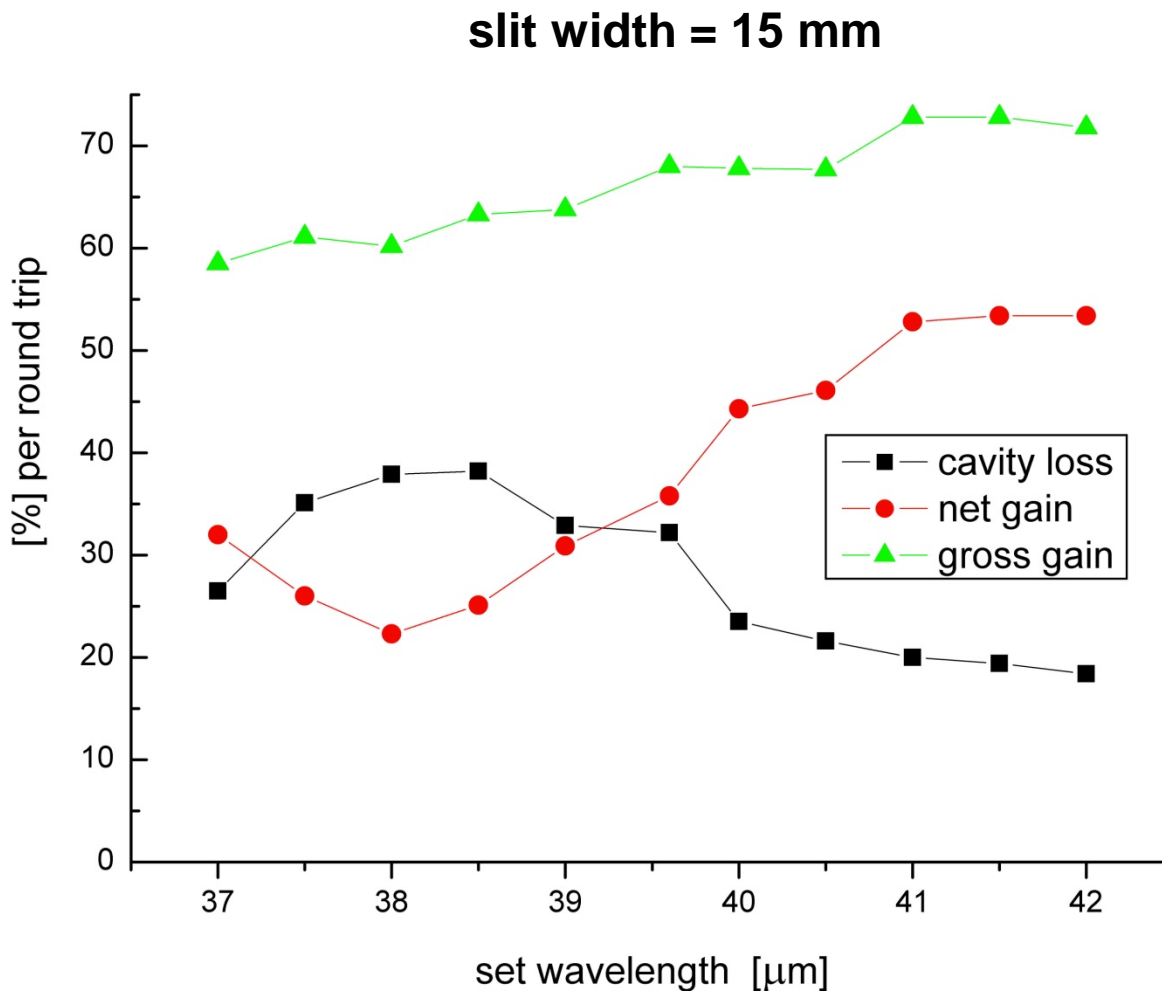
Mode conversion in free-space part



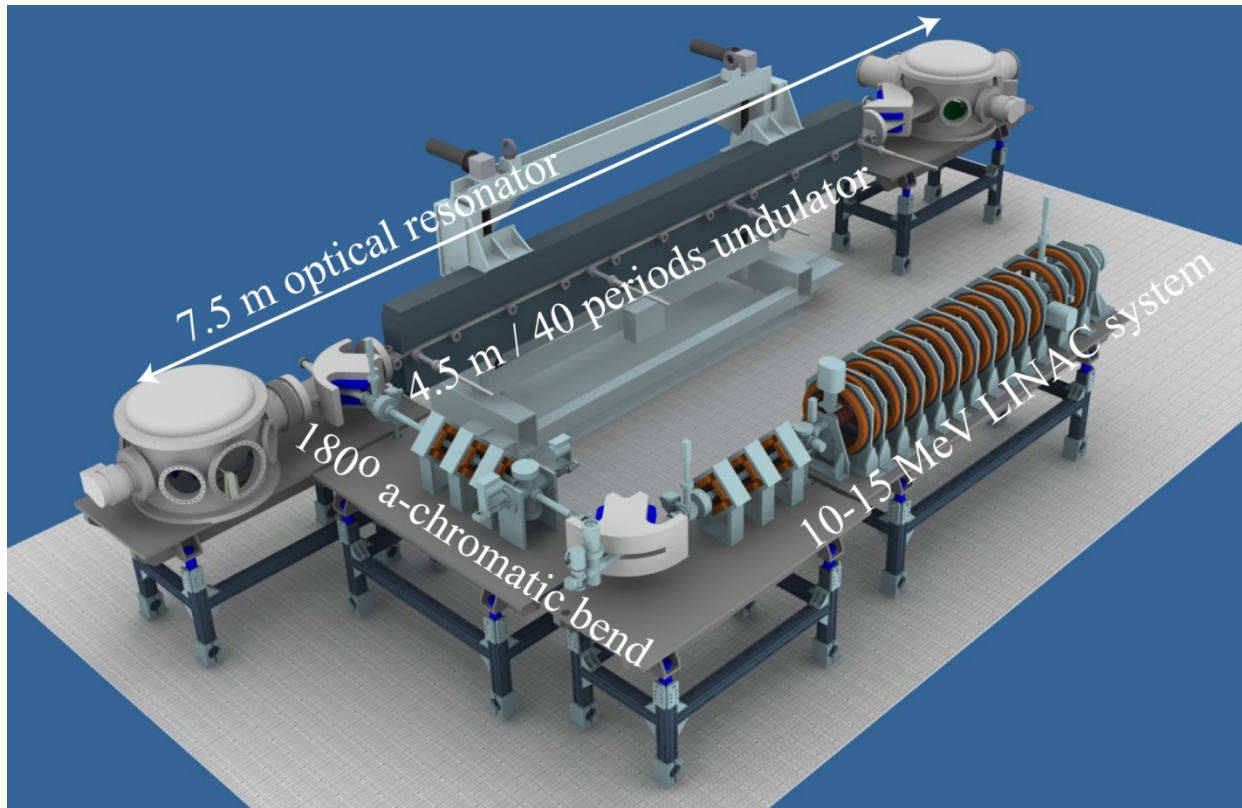
Measured roundtrip gain and loss



Measured roundtrip gain and loss cont.

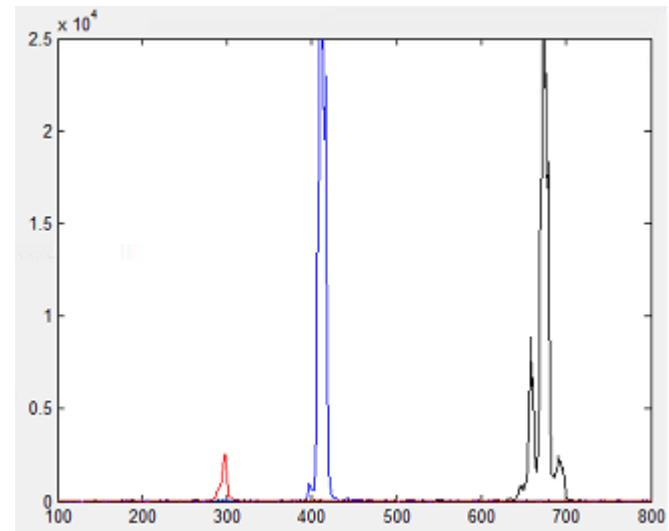
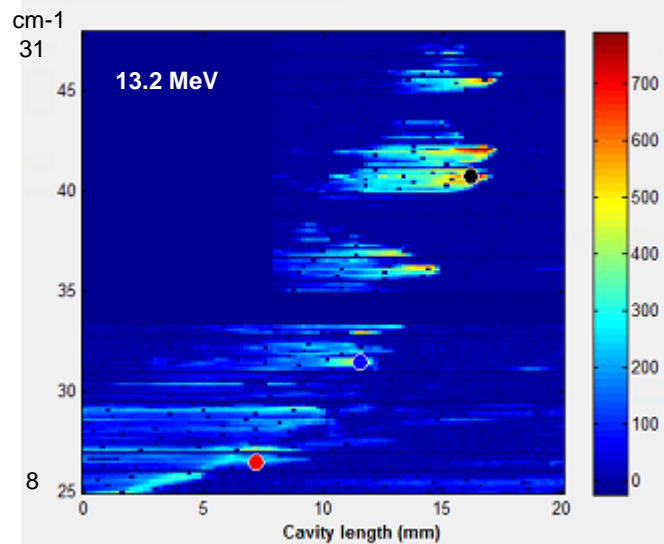
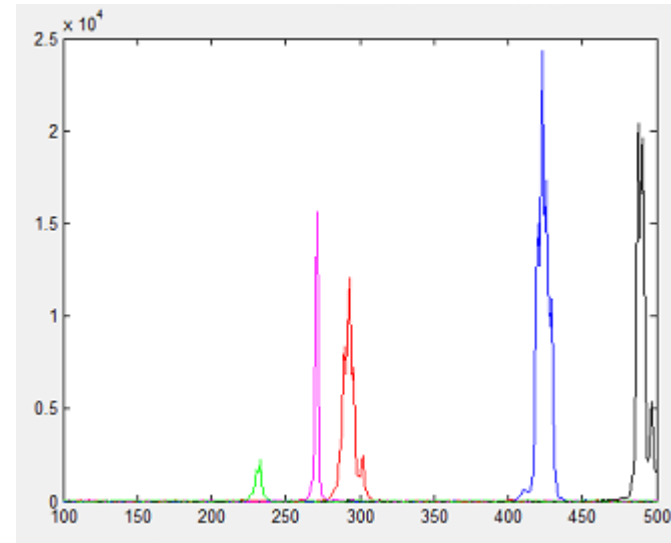
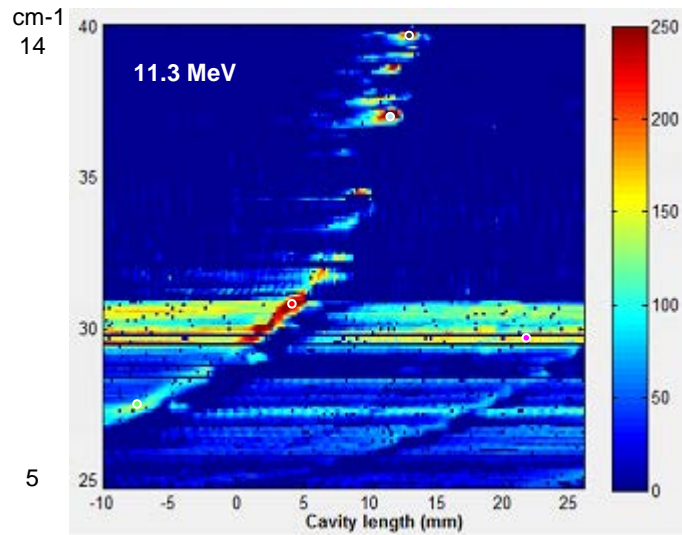


'FLARE' in Nijmegen



e-beam: 10-15 MeV, 3 GHz, 10 μ s, 10 Hz
wavelength range: 100 – 1500 μ m
special feature: narrow-band mode

FLARE tuning gaps

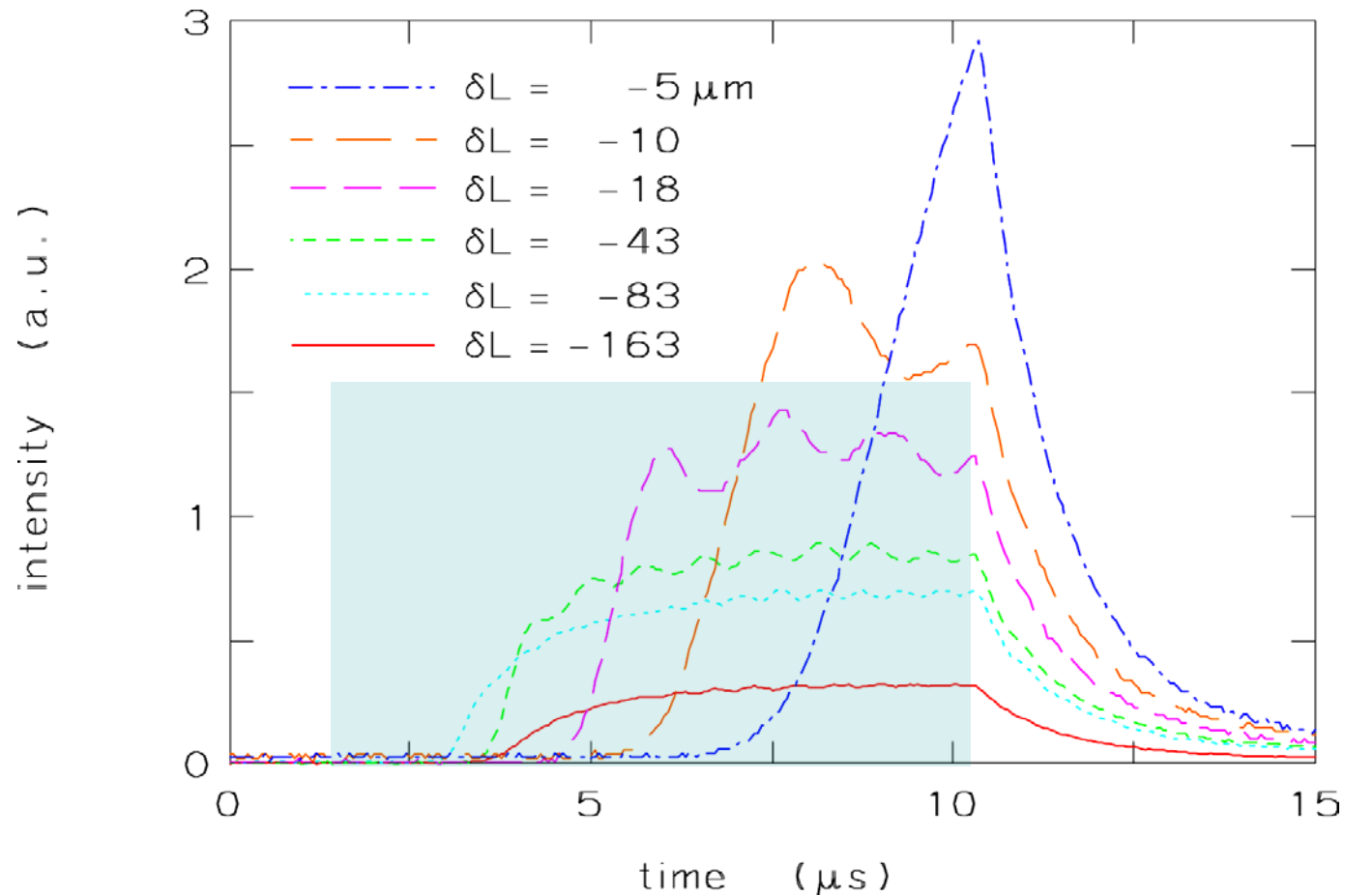


Slippage effects

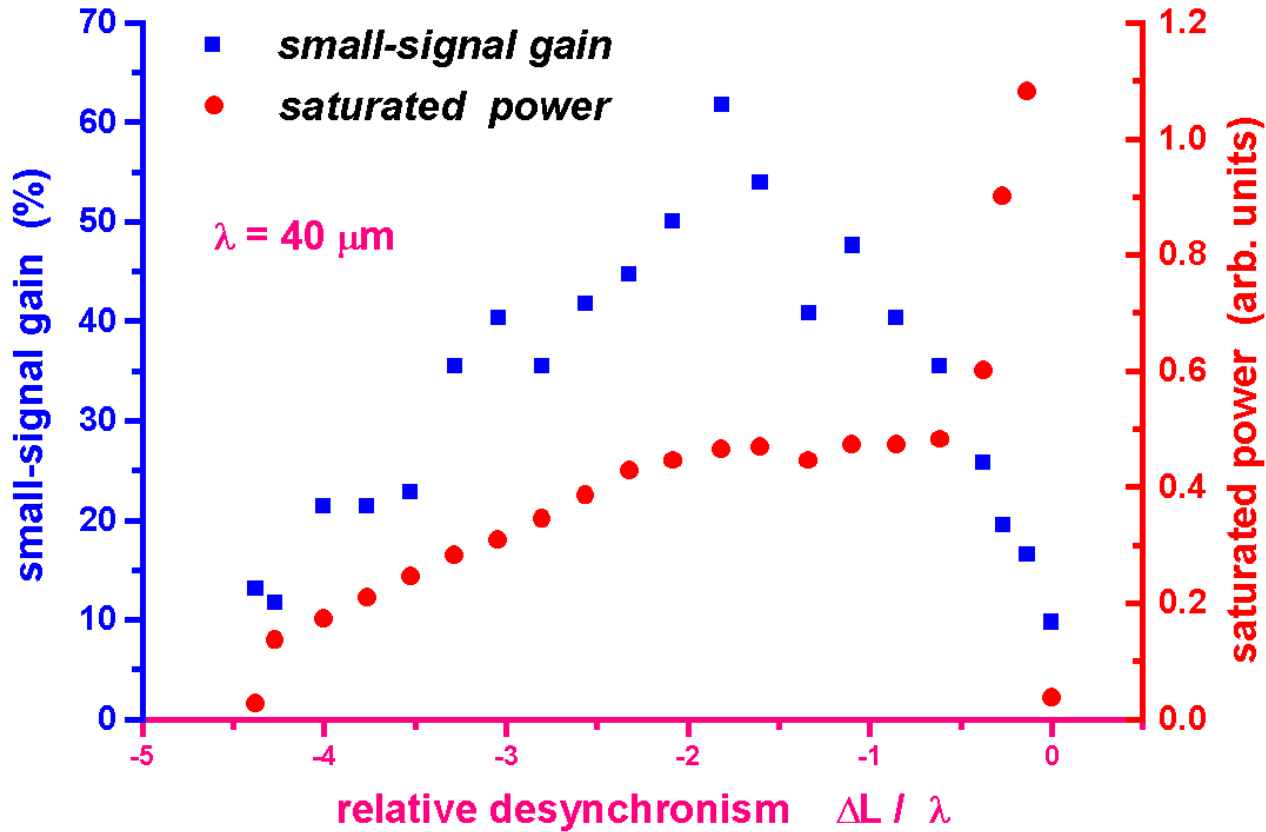
- Lethargy
- Efficiency enhancement
- Limit-cycles
- Bandwidth tuning

Slippage effects

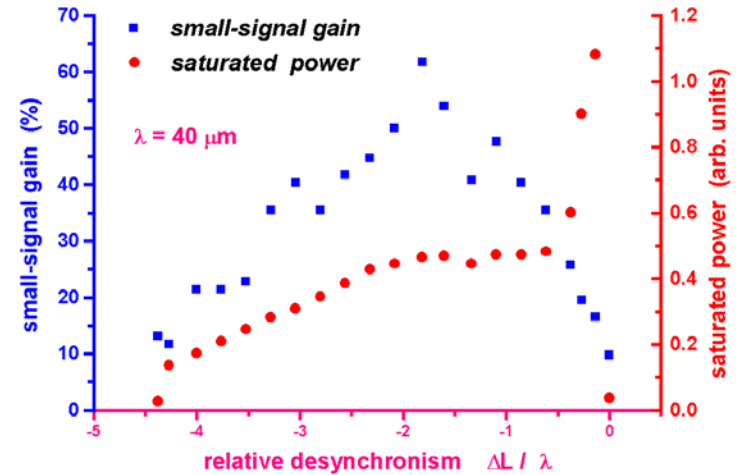
FELIX macropulse shape at $\lambda = 40 \mu\text{m}$



Slippage effects: gain and saturation



Slippage effects: gain and saturation

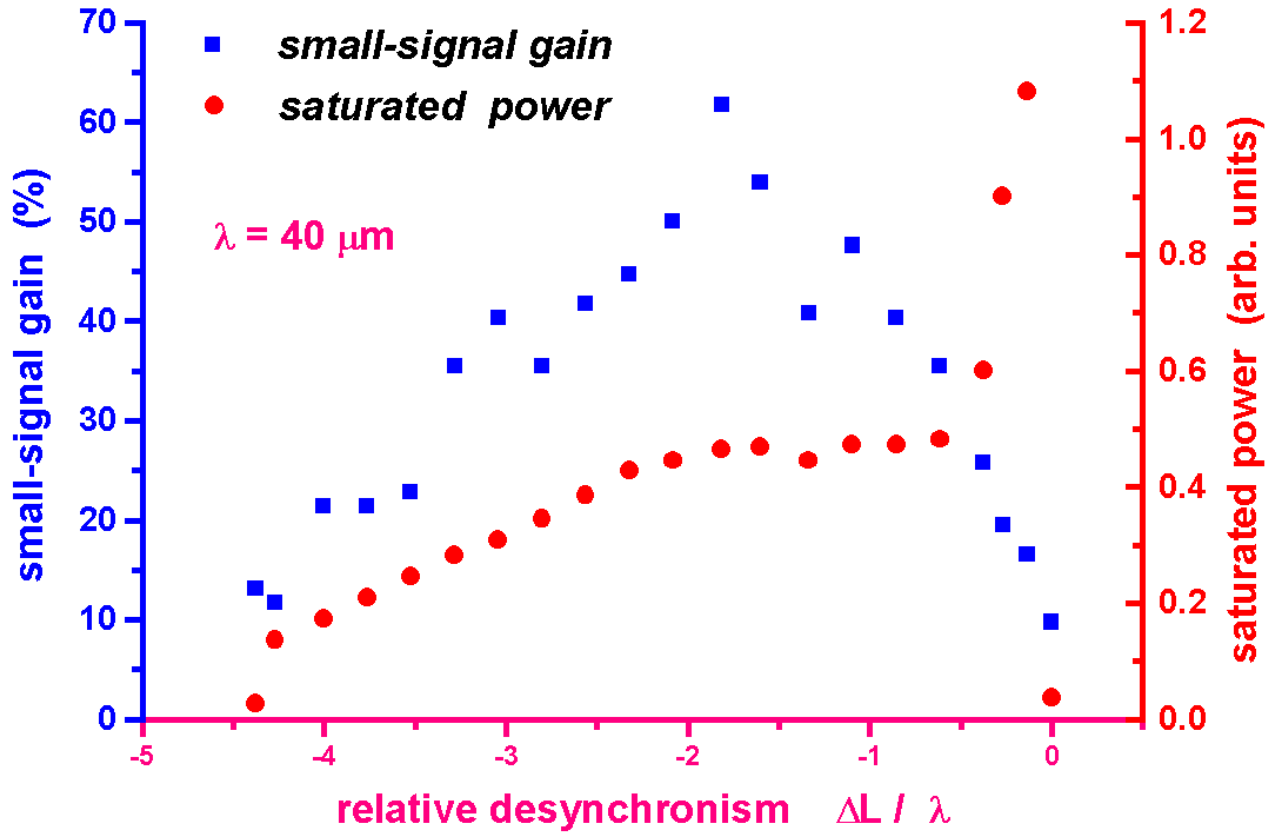


Slippage correction:

$$g_o \longrightarrow \text{Gain} \sim \frac{g_o}{\left(1 + \frac{N_u \lambda}{3\sigma_z}\right)}$$

$$g_o \sim I \sim \frac{Q_b}{\sigma_z} \longrightarrow \text{Gain} \sim \frac{Q_b}{\left(\sigma_z + \frac{N_u \lambda}{3}\right)}$$

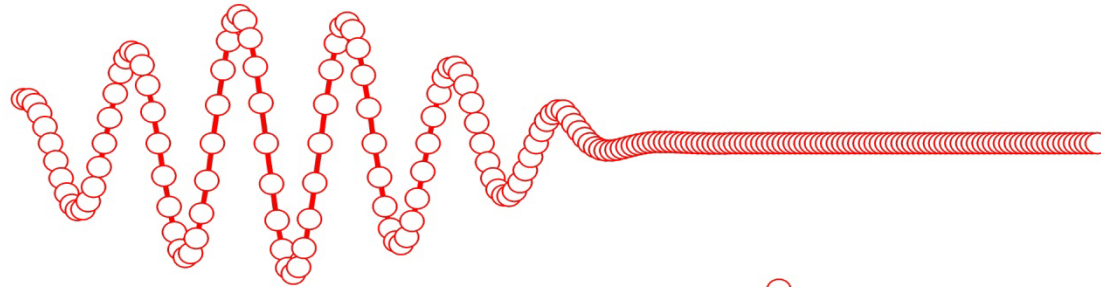
Slippage effects: gain and saturation



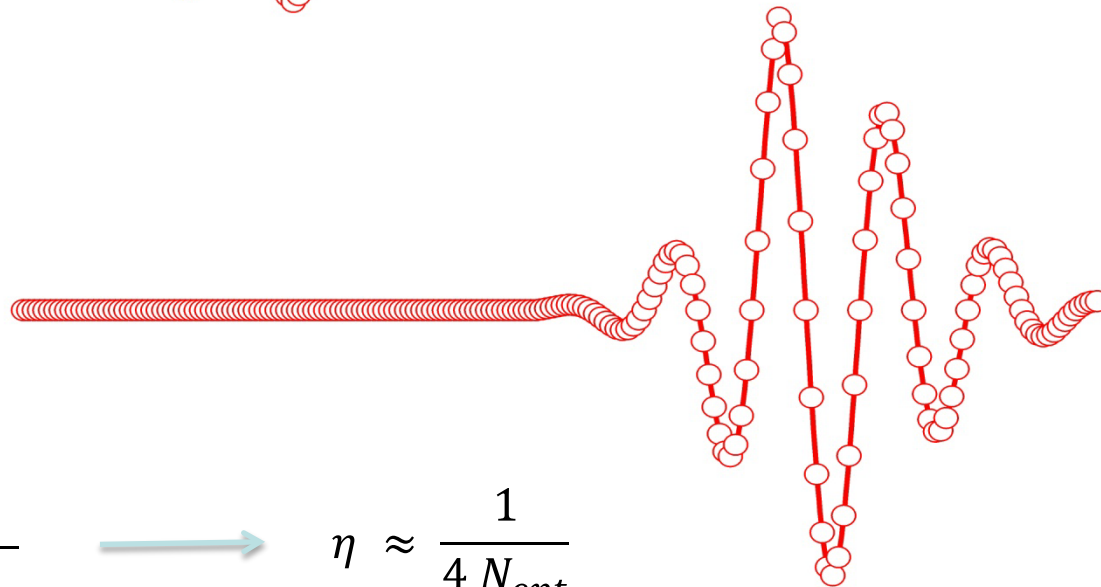
Slippage effects: efficiency enhancement

short pulse propagation

entrance



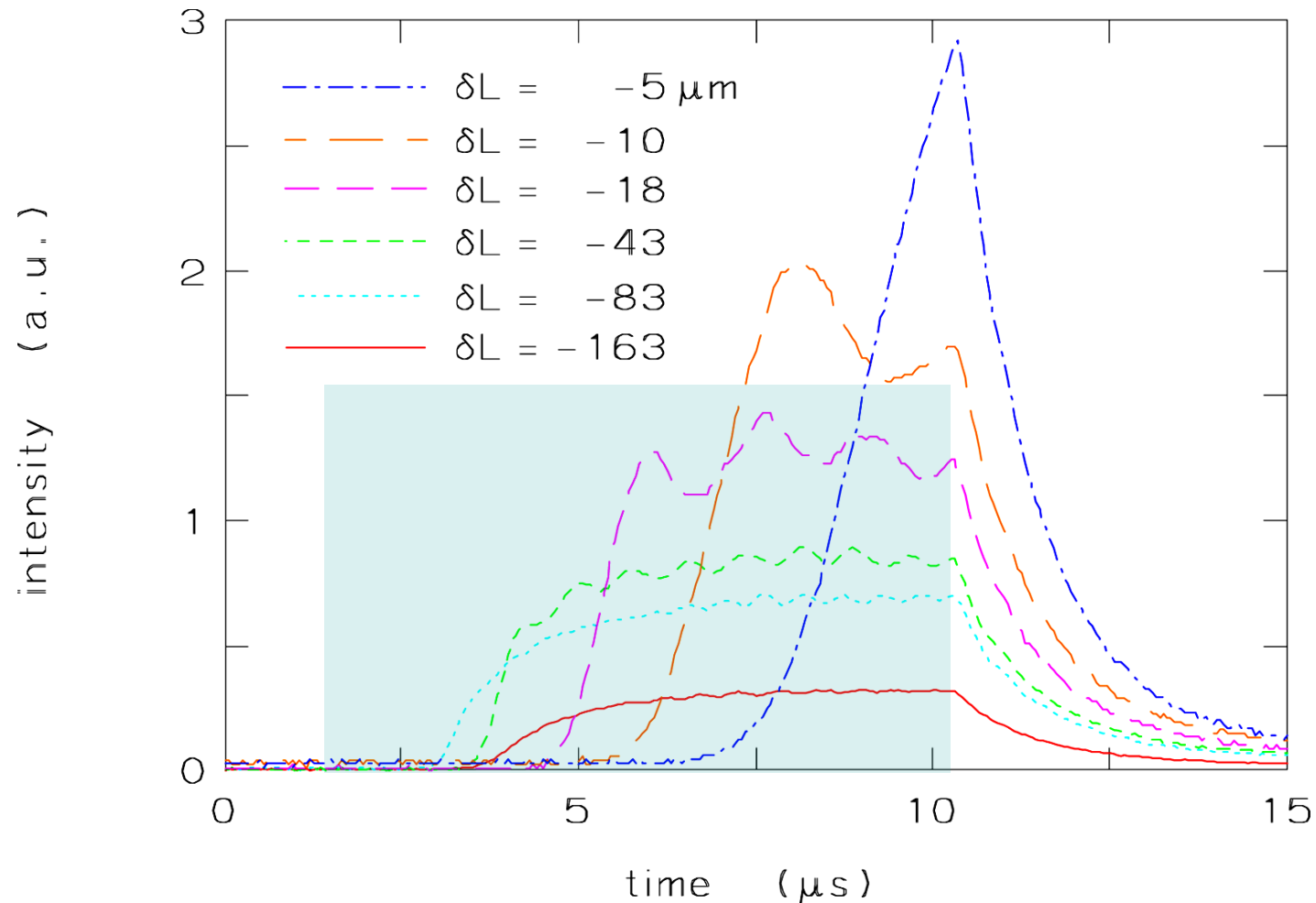
exit



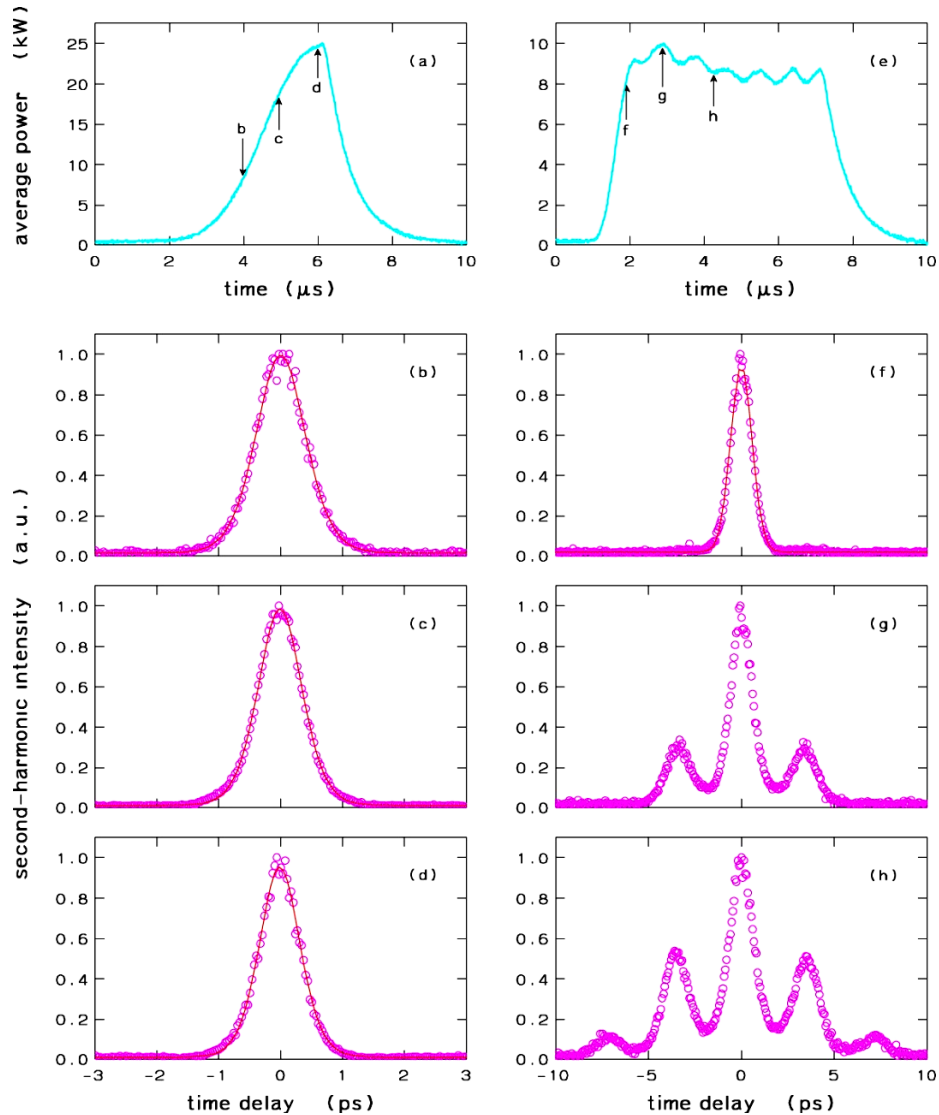
$$\eta \approx \frac{1}{4 N_u} \longrightarrow \eta \approx \frac{1}{4 N_{opt}}$$

Slippage effects

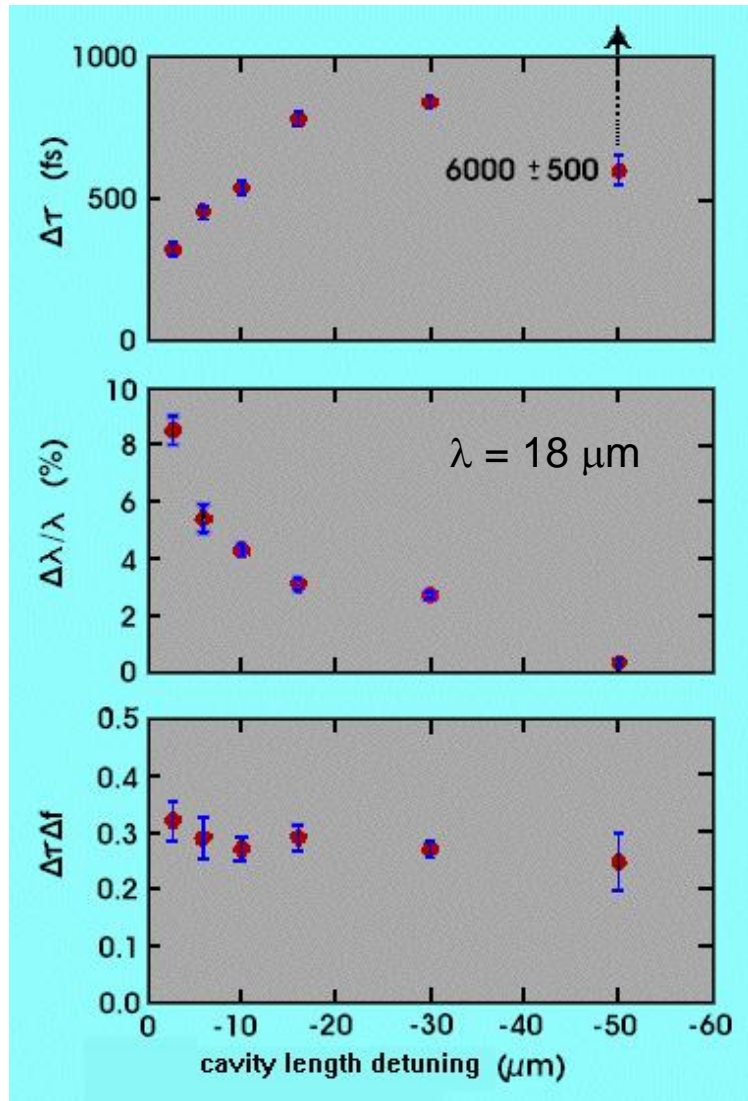
FELIX macropulse shape at $\lambda = 40 \mu\text{m}$



Slippage effects: limit cycles



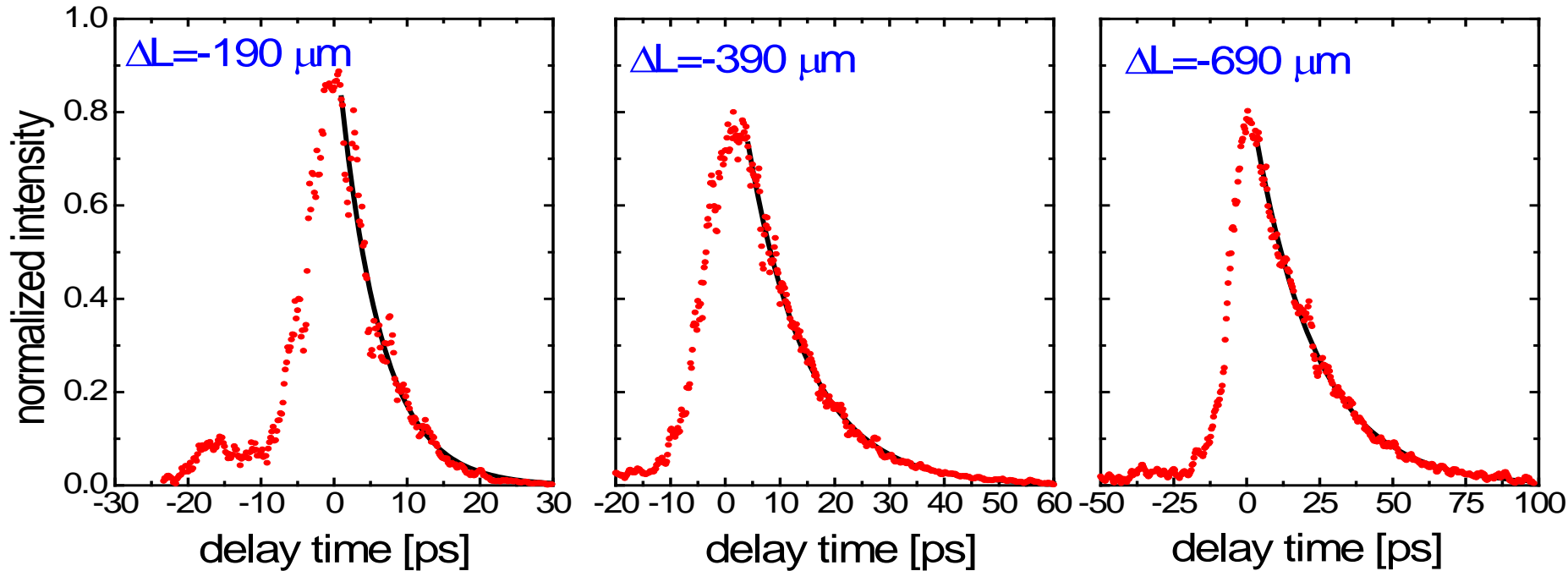
Slippage effects: bandwidth tunability



- bandwidth 0.4 - 6% [FWHM]
- near transform limited

Slippage effects: pulse length tunability

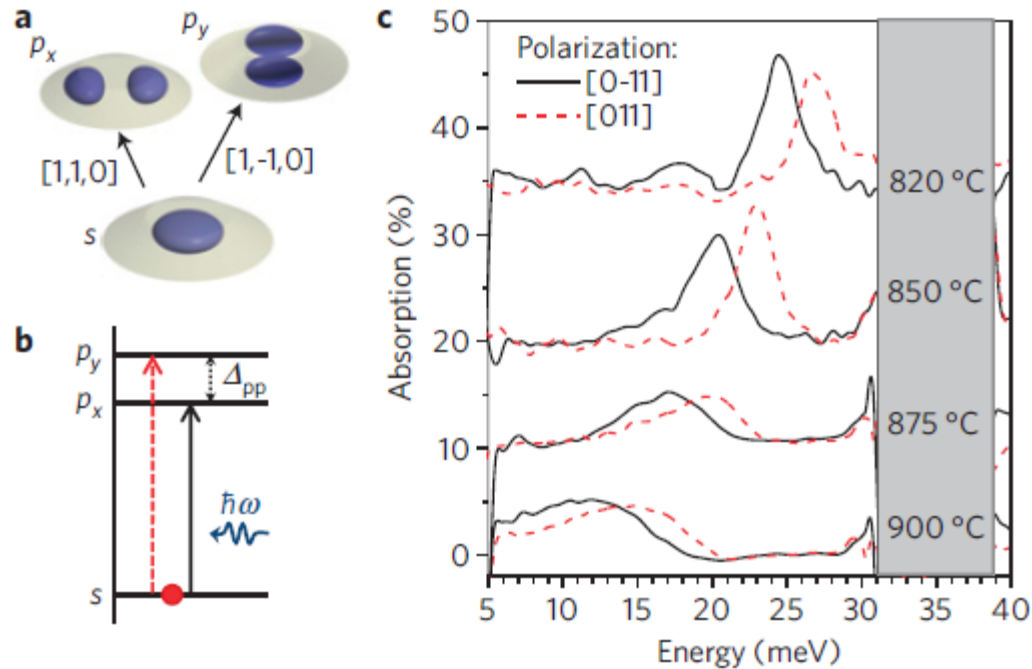
FELIX micro-pulse shape at $\lambda = 150$ mm
for different cavity detunings



Exponential **leading** edge has a time constant:
where α are the cavity losses and ΔL is the
cavity detuning from synchronism

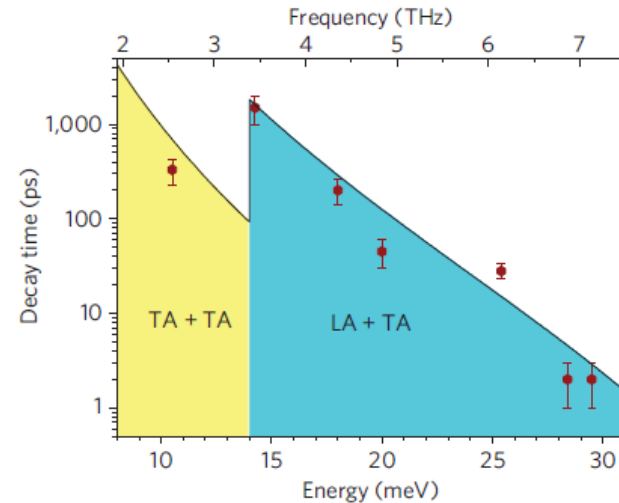
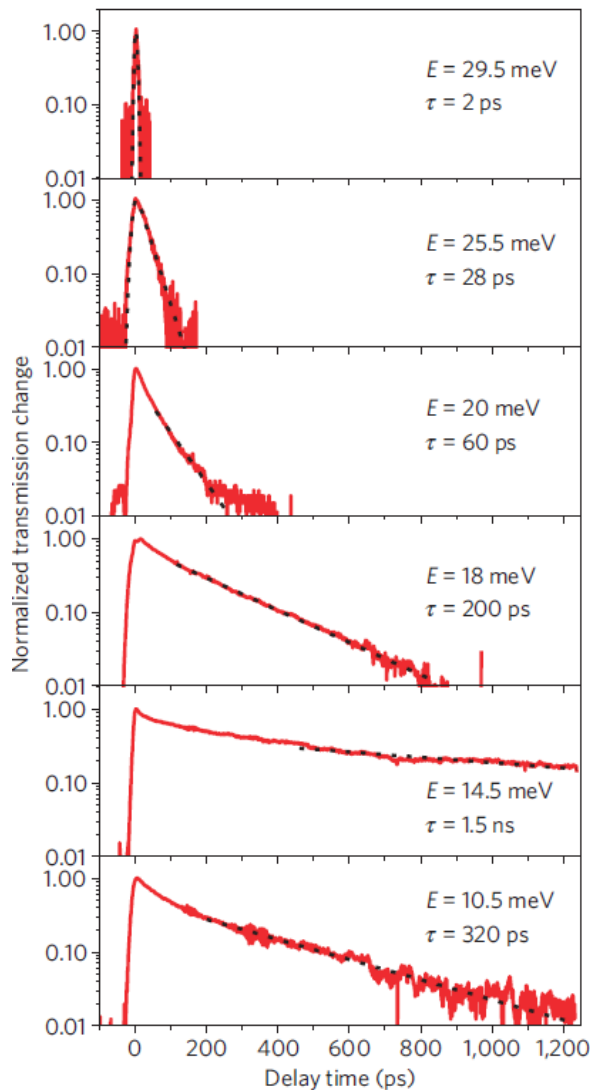
$$\tau = \frac{2\Delta L}{\alpha c}$$

Nonlinear optics: lifetime of quantum-dot intersubband levels



InGaAs self-assembled quantum dots

Nonlinear optics: lifetime of quantum-dot intersubband levels

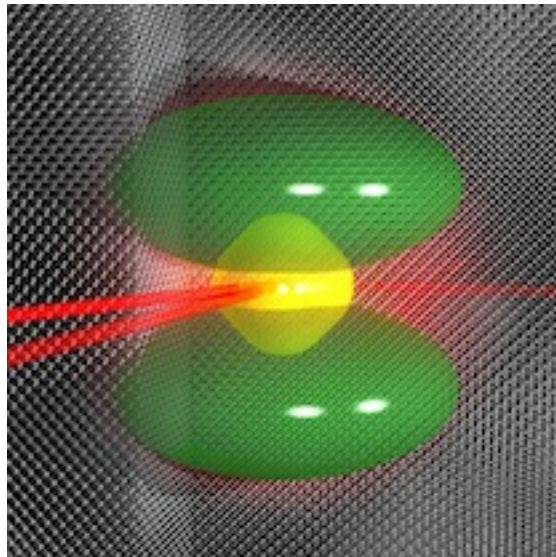


Lifetime strongly depends on energetically available decay channel

FELBE: E.Zibik et al., Nature Materials 8 (2009) 803

A hydrogen-like atom in a silicon chip

The periodic table shows the positions of Silicon (Si) and Phosphorus (P). Silicon is located in group 14, period 3, and Phosphorus is in group 15, period 3. Both elements are highlighted with red boxes.



- Binding energy:

$$E_R = \frac{1}{2} \left(\frac{e^2}{2h} \right)^2 \frac{m_e}{\epsilon^2}$$

- Bohr radius

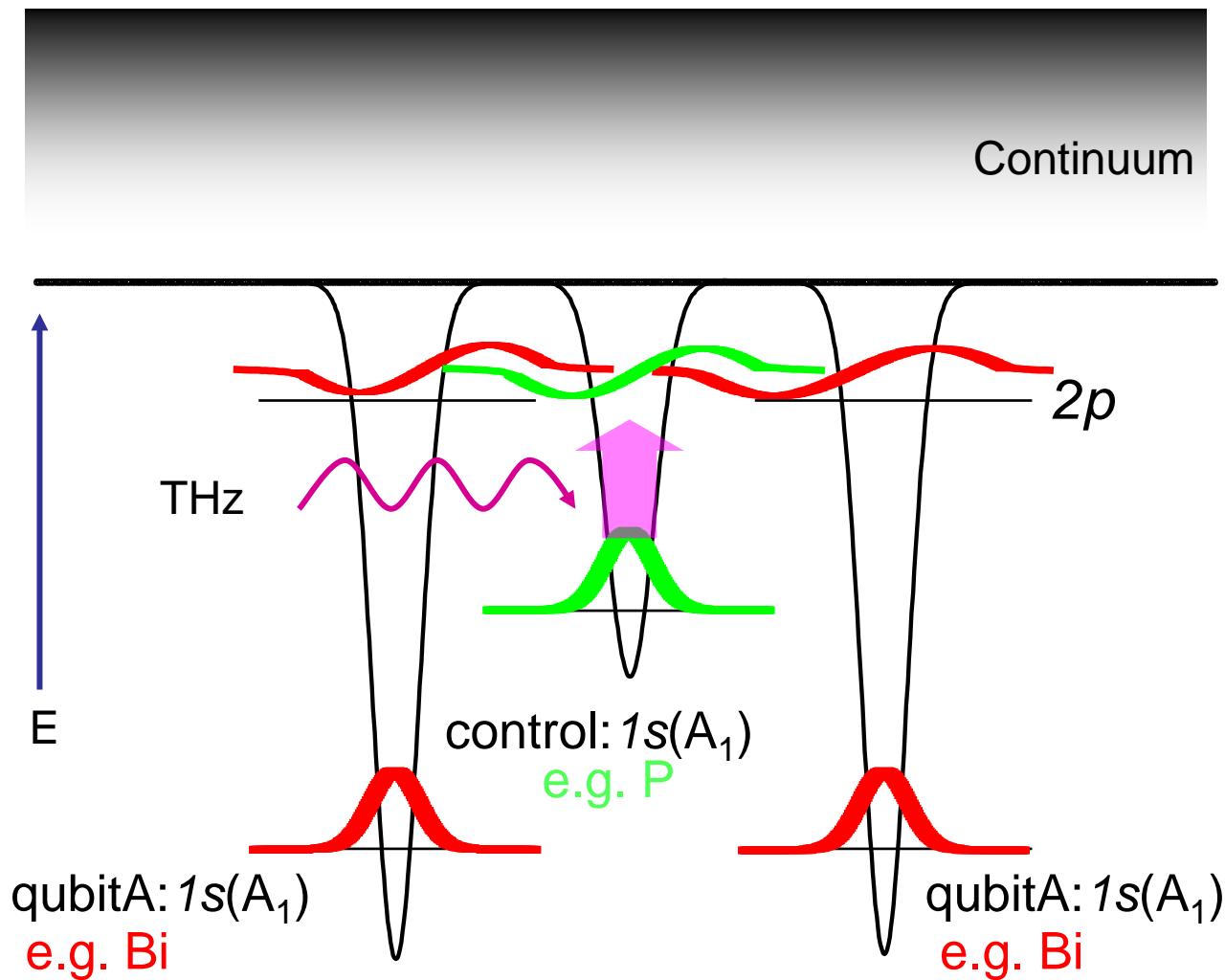
$$a_0 = \frac{h^2}{\pi \cdot e^2} \frac{\epsilon}{m_e}$$

- Characteristic field

$$B_0 = \frac{\pi}{4} \left(\frac{e}{h} \right)^3 \frac{m_e^2}{\epsilon^2}$$

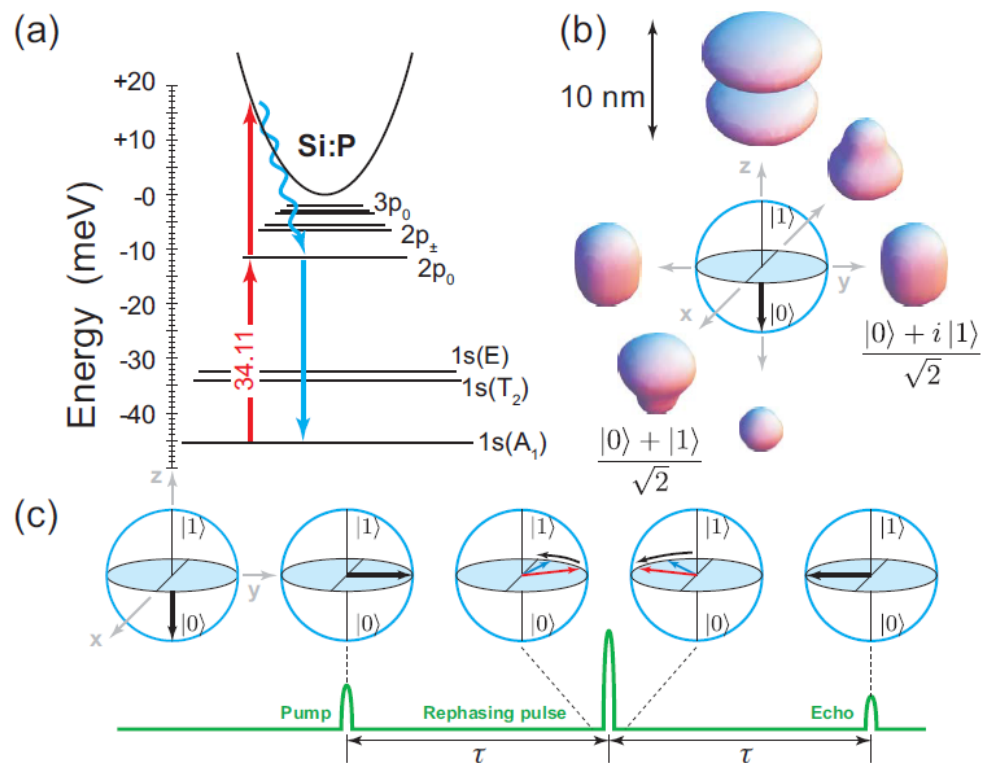
	H	Si:P
ϵ_r	1	11.4
m_e	1	0.19
E_R	13.6 eV	0.020 eV
a_0	0.056 nm	3.2 nm
B_0	117,000 T	32 T

QIP proposal: THz control of entanglement

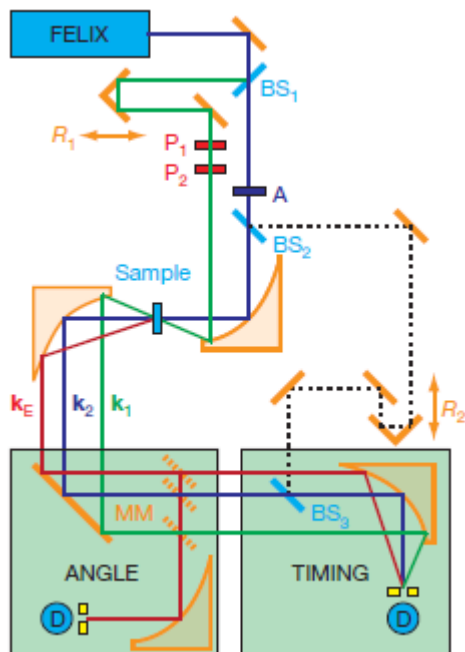


A. M. Stoneham *et al*, *J. Phys. C*, 15, L447, 2003.

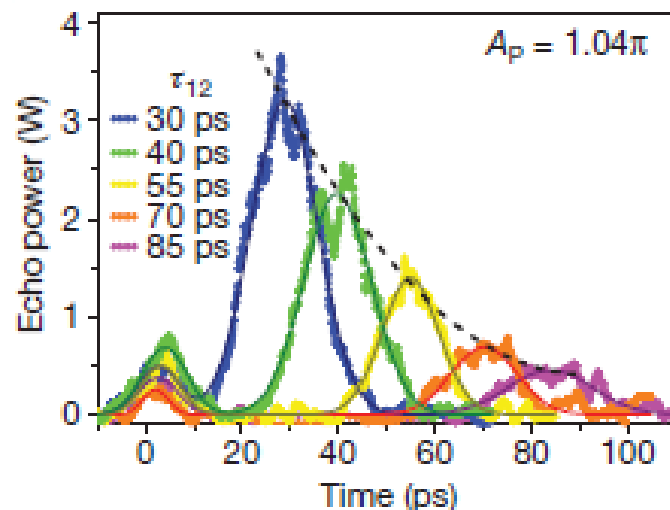
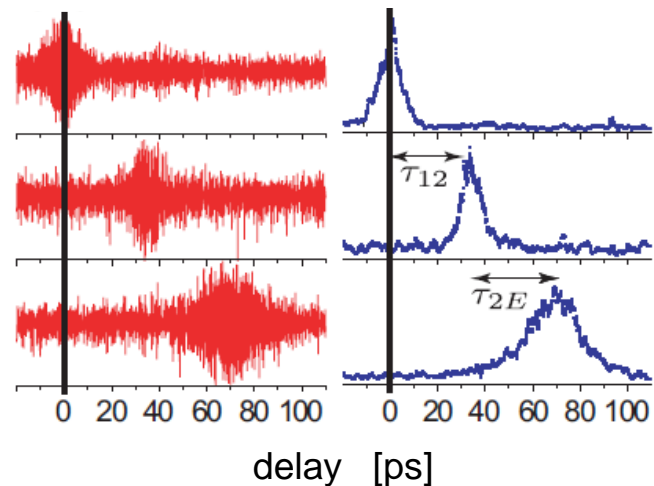
Coherent control of orbital states: Hahn echo in Si:P



Coherent control of orbital states: Hahn echo in Si:P

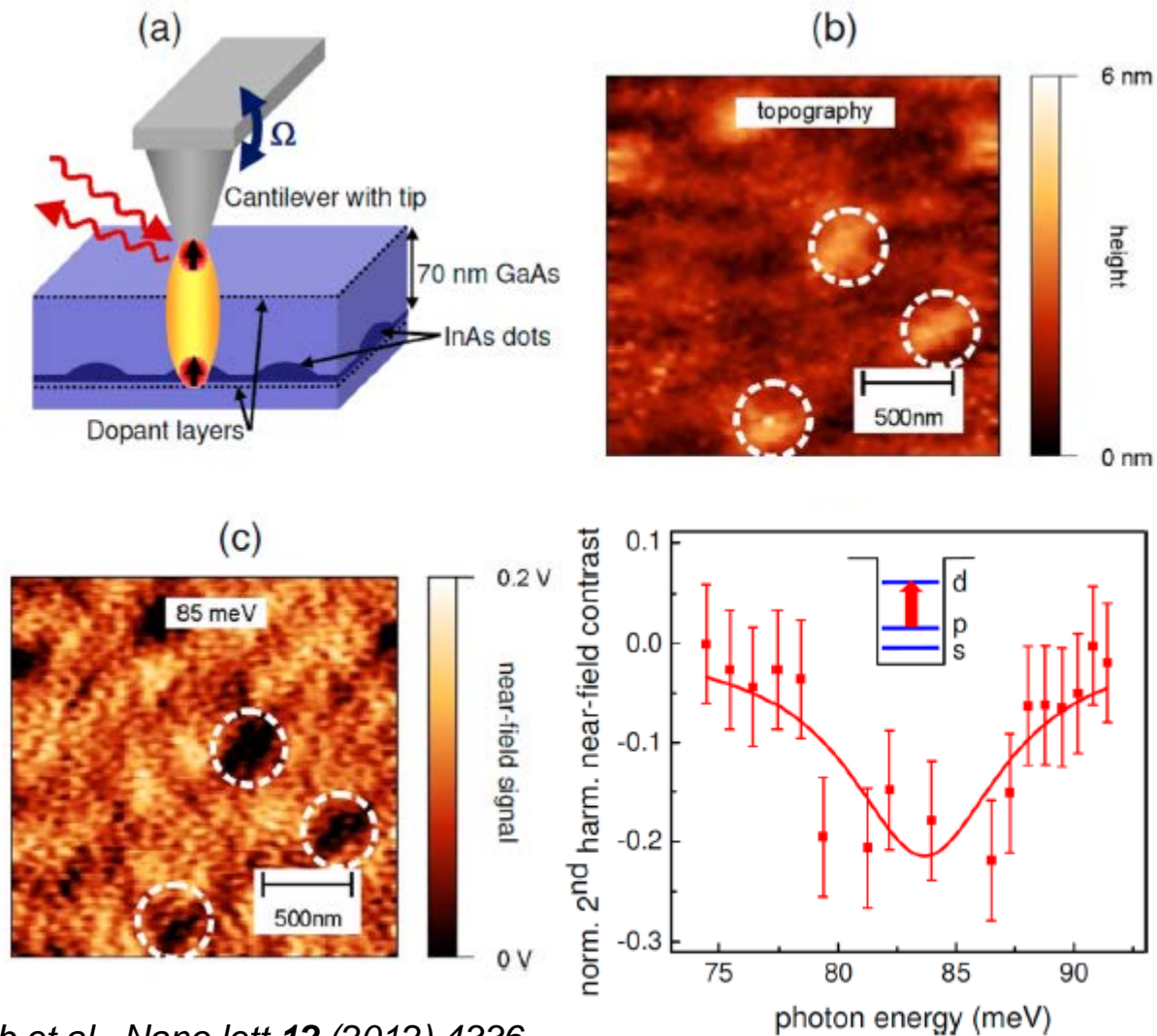


$T_2 \sim 160$ ps lifetime



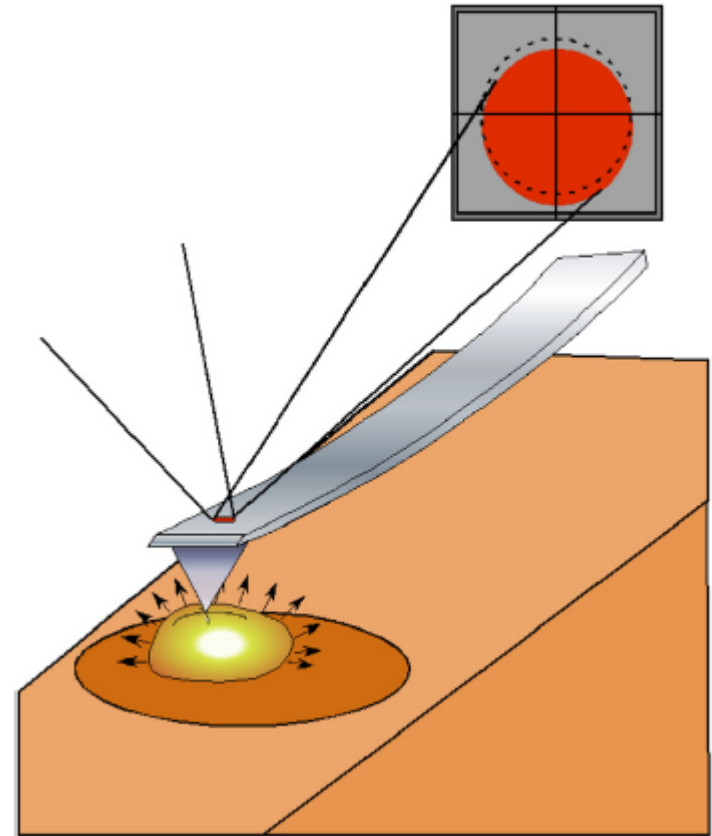
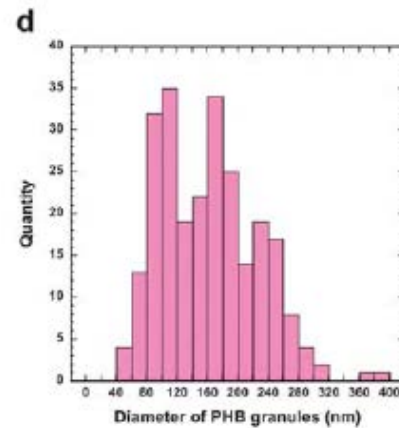
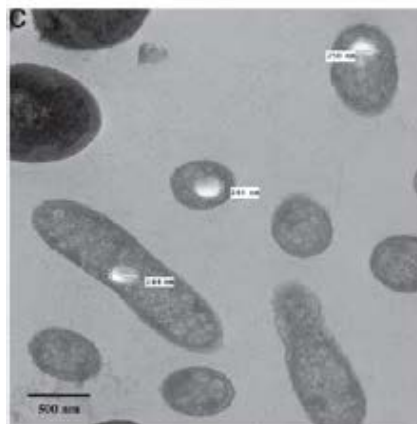
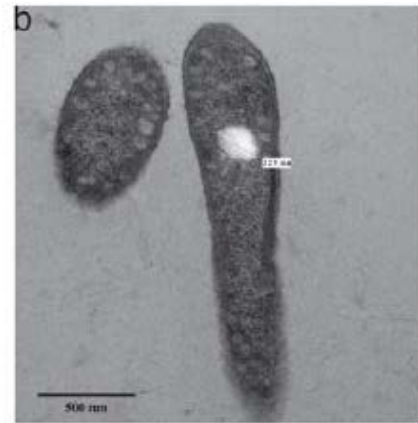
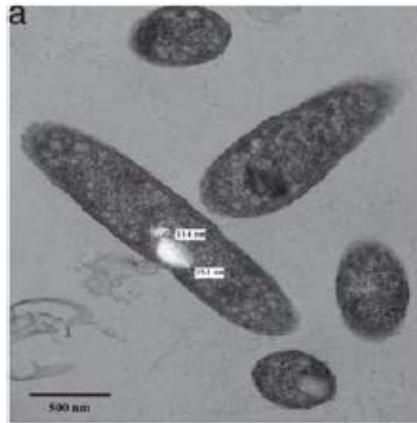
Greenland et al, Nature **465** (2010) 1057

Nano spectroscopy: single quantum dot

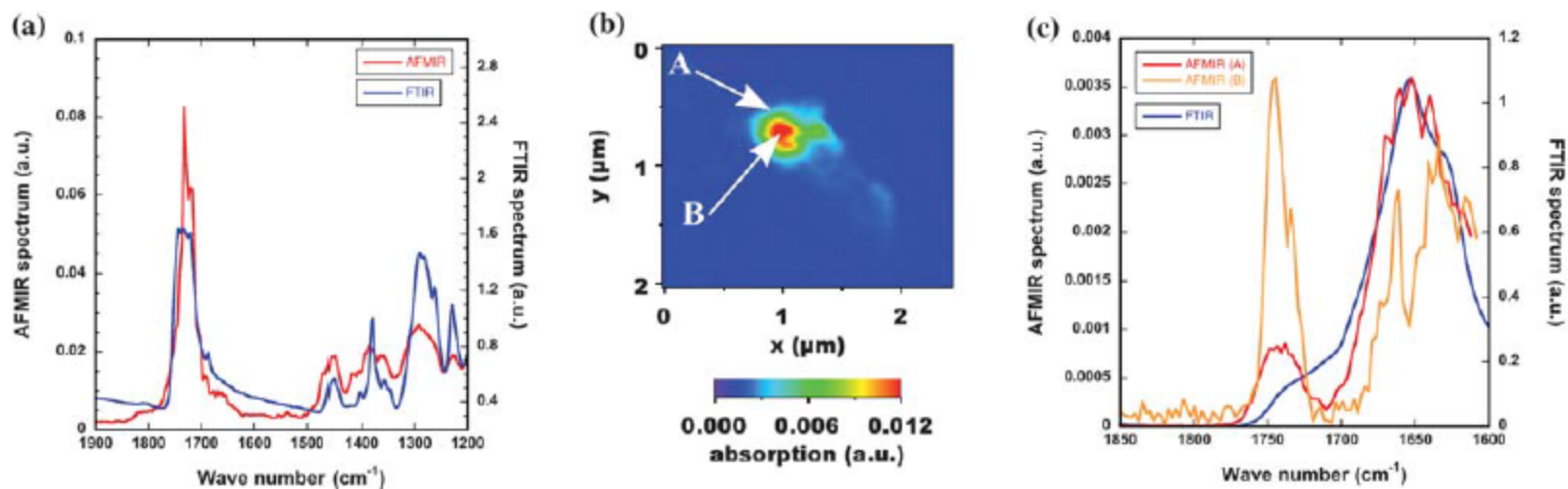


FELBE: R. Jacob et al., *Nano lett.* **12** (2012) 4336

Nano spectroscopy: PHB inside bacteria



Nano spectroscopy: PHB inside bacteria



CLIO: C. Mayet et al., *Analyst* **135** (2010) 2540

Nano spectroscopy: spin-off

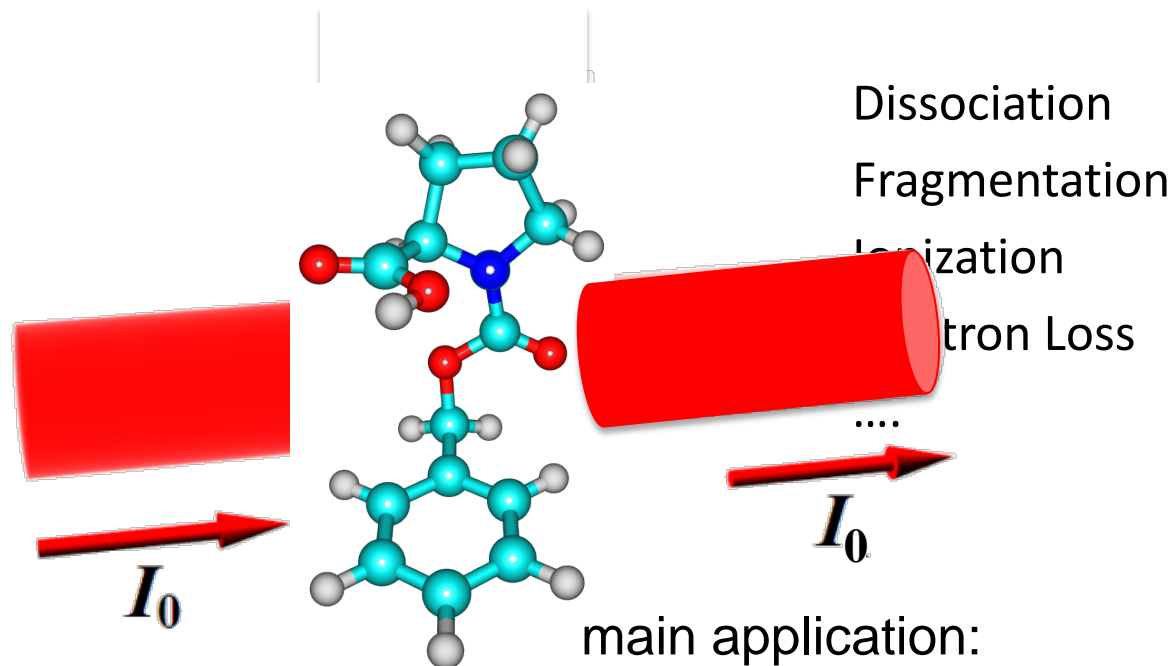
nanoIR2™ from the world leader in nanoscale IR spectroscopy

The complete nanoscale IR spectroscopy solution for all your material analysis needs.
The nanoIR2, the only platform that offers:

- AFM-IR for soft materials, including organics, polymers, composites and life sciences
- True, model-free spectroscopic chemical analysis with AFM-IR – not ambiguous material mapping
- Proven ease of use and productivity on real world samples
- Powerful, full-featured AFM with standard imaging modes

ANASYS
INSTRUMENTS
The nanoscale analysis company

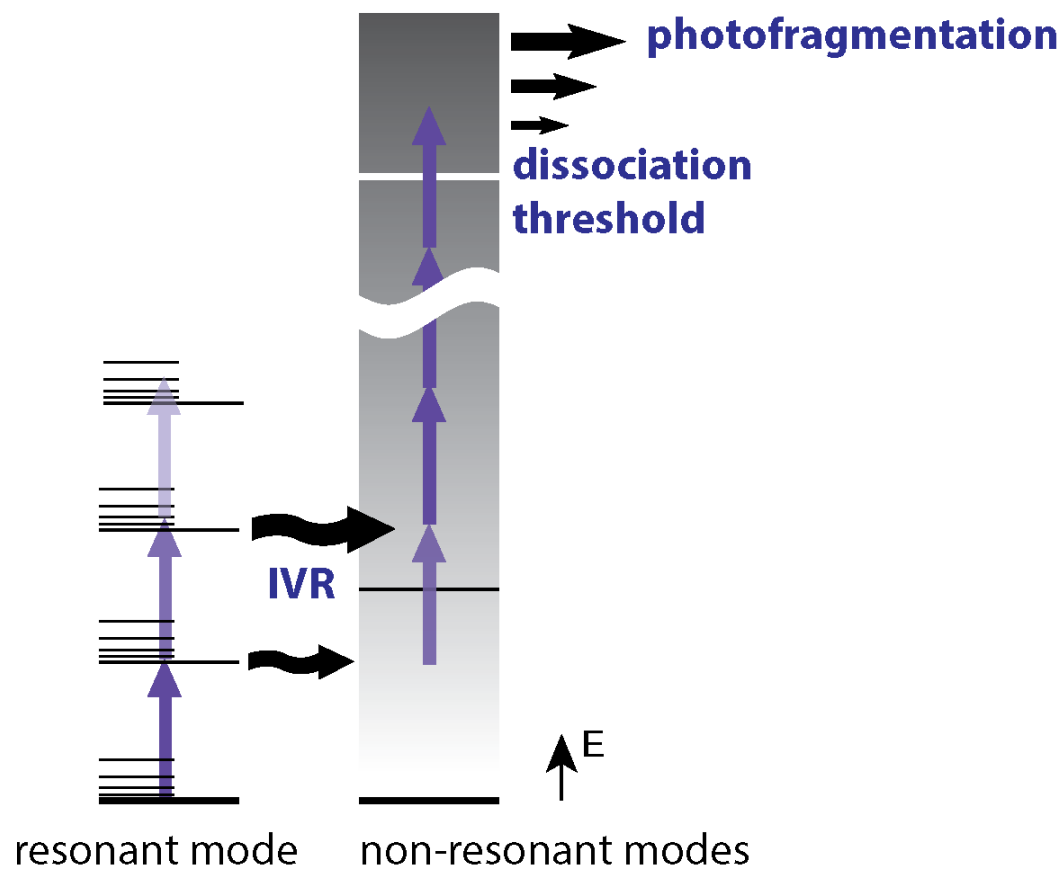
Infrared Action Spectroscopy



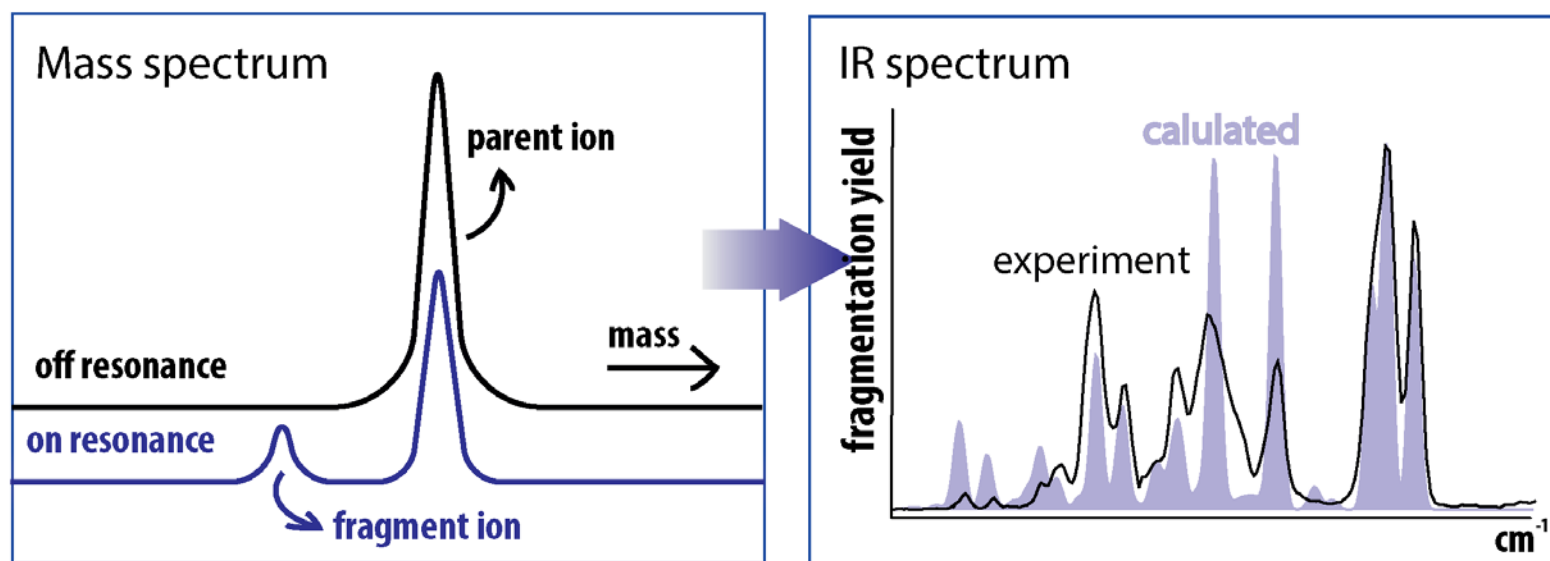
Dissociation
Fragmentation
Ionization
Electron Loss
....

main application:
gas phase studies
molecules, clusters, complexes
neutral, ionic species
molecular beams, ion traps

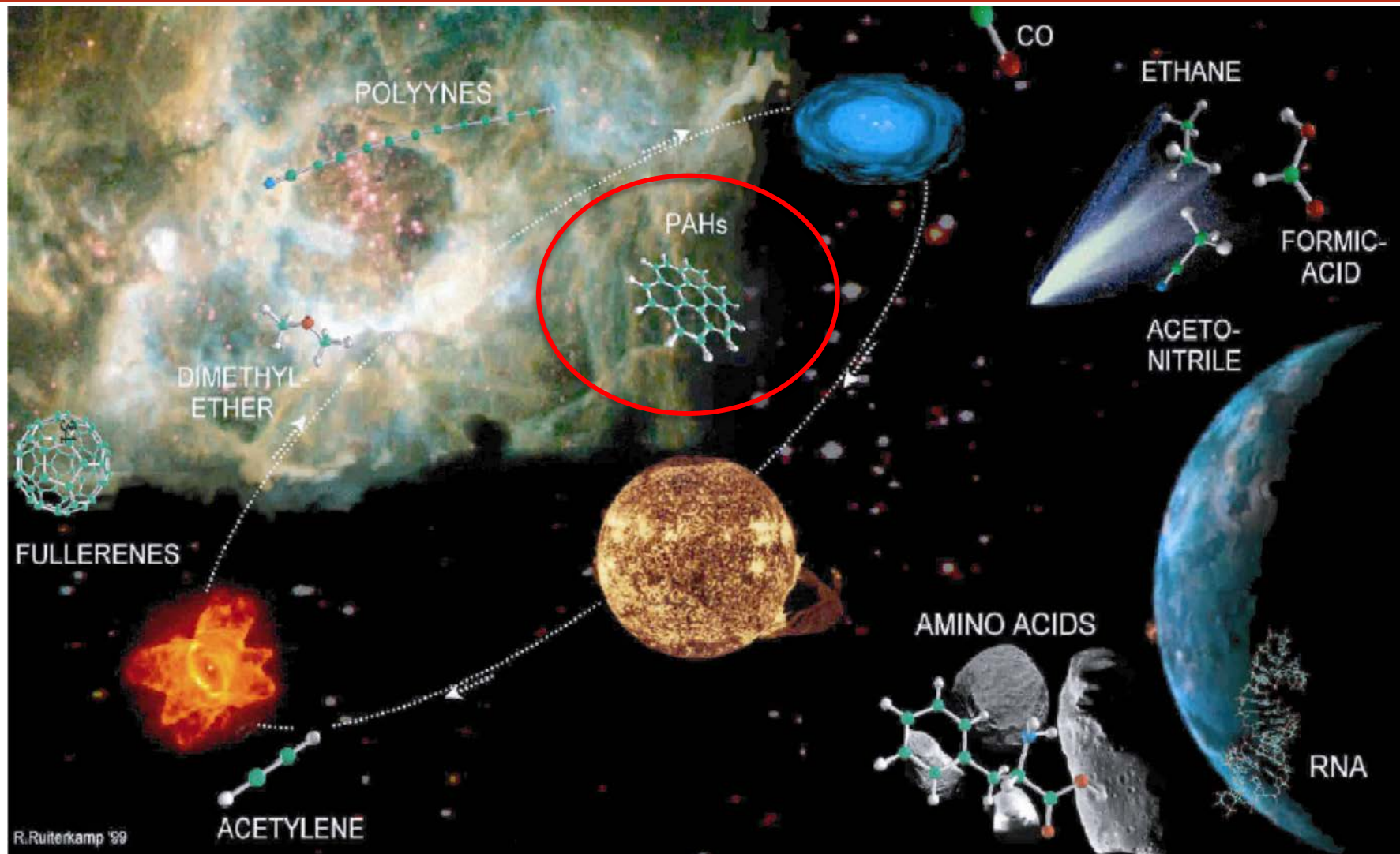
Mechanism, Infrared Spectrum, Molecular Structure



Mechanism, Infrared Spectrum, Molecular Structure

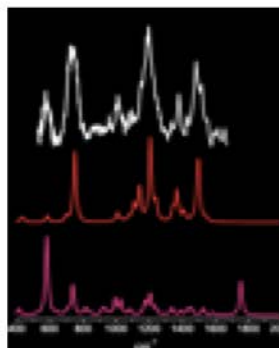
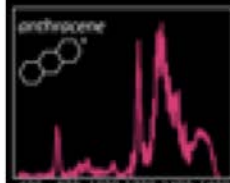
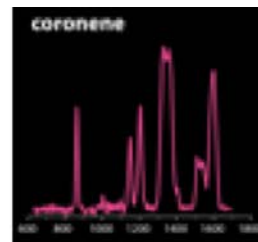
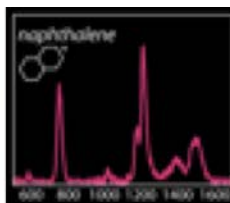
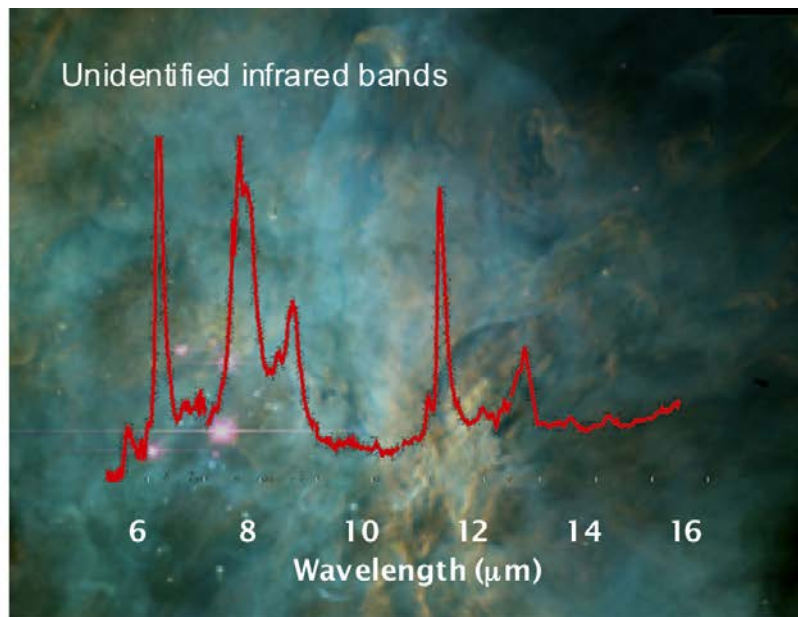


Large organic compounds in space

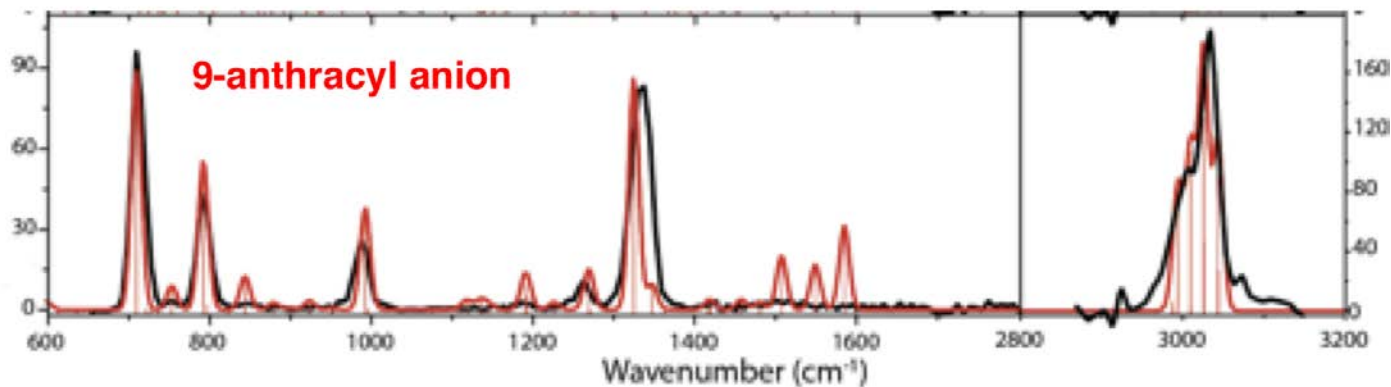


P. Ehrenfreund

Gas-phase infrared spectra of ionic PAHs

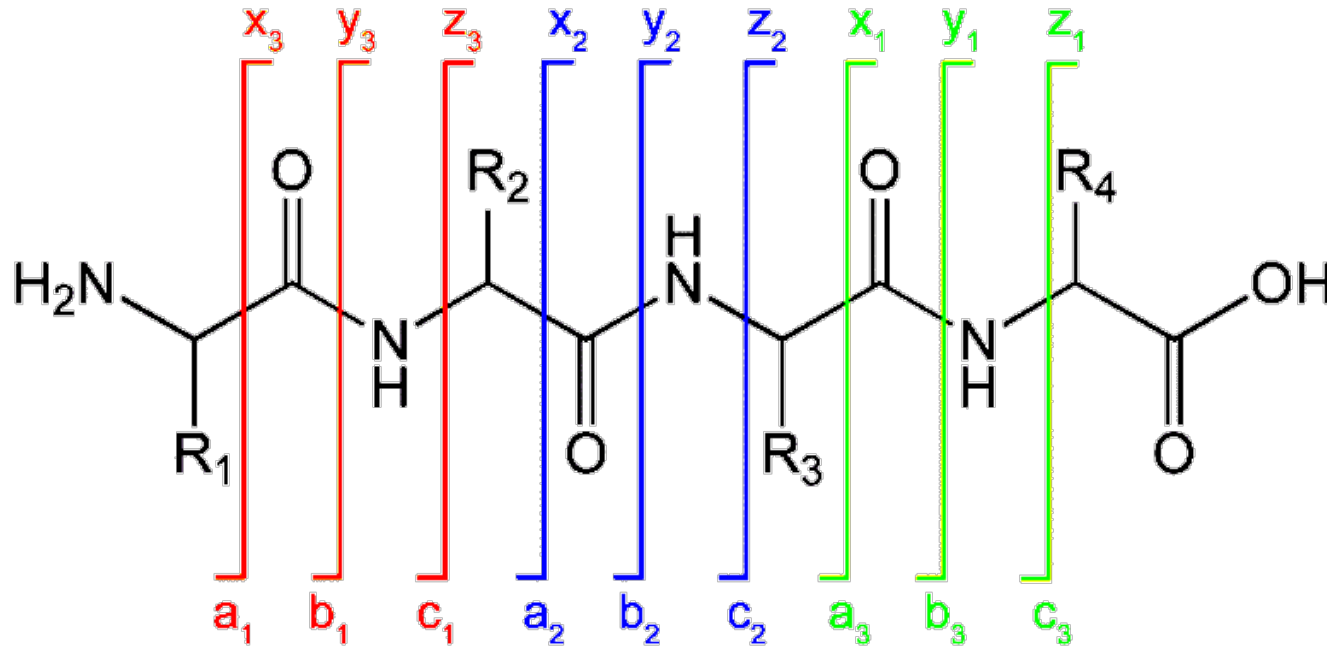


ApJ **542** 404 (2000)
ApJL **560** L90 (2001)
JPC-A **105** 8302 (2001)
JPC-A **107** 782 (2003)
ApJ **591** 968 (2003)
ApJ L66 706 (2009)
JCP 131 184307 (2009)
ANIE 50 7004 (2011)
ApJ 83 746 (2012)
ApJ 170 787 (2014)
.....

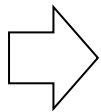


- Investigate various and larger systems in various states – cation, anion, protonated, deprotonated etc.

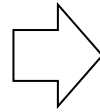
Understanding Mechanisms of Peptide sequencing



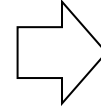
collisional
activation



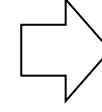
mobile
proton



nucleophilic
attack

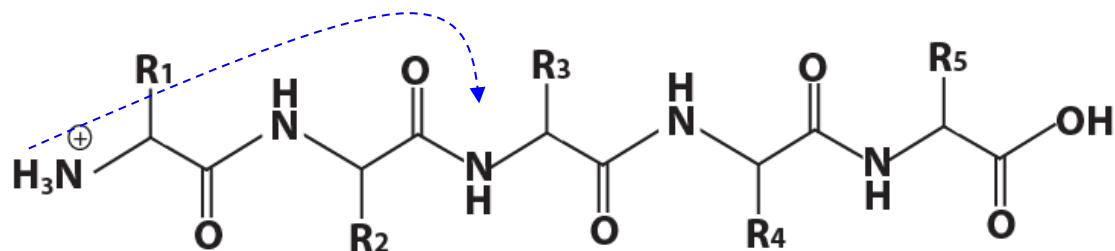


amide bond
cleavage

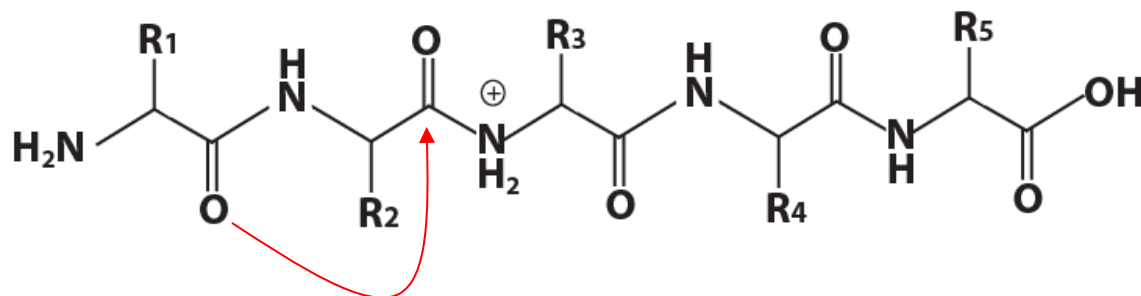


b/y
fragments

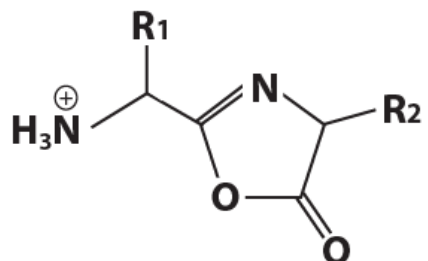
b/y fragmentation pathway



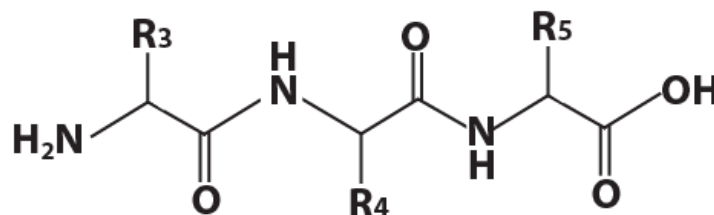
mobile proton



nucleophilic attack



b-fragment: oxazolone



amide bond cleavage

y-fragment: truncated peptide

Do all b_2 ions have oxazolone structures?



ELSEVIER

International Journal of Mass Spectrometry 210/211 (2001) 71–87



www.elsevier.com/locate/ijms

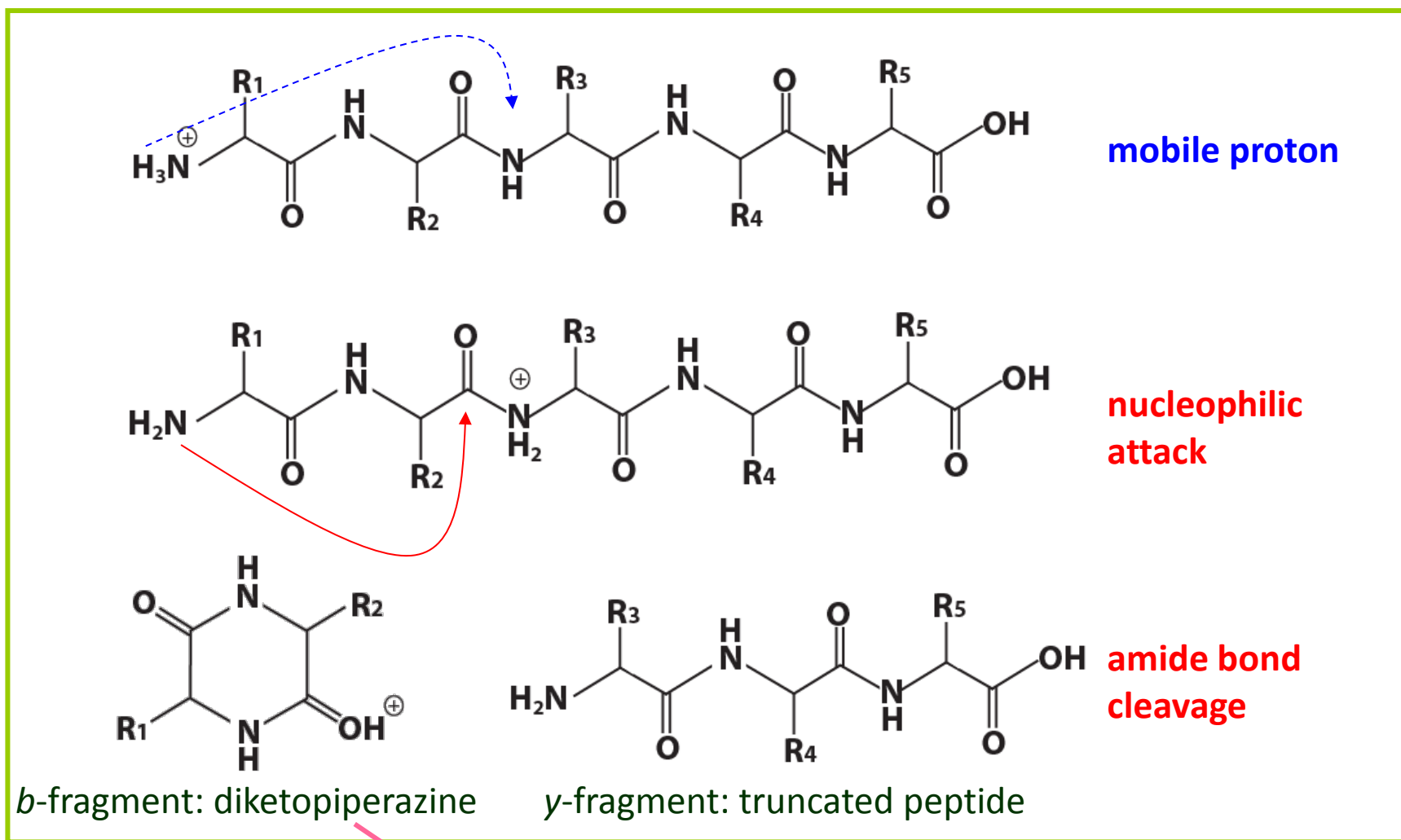
Do all b_2 ions have oxazolone structures? Multistage mass spectrometry and ab initio studies on protonated *N*-acyl amino acid methyl ester model systems[†]

Jason M. Farrugia, Richard A. J. O'Hair*, Gavin E. Reid¹

School of Chemistry, University of Melbourne, Victoria 3010, Australia

Received 5 December 2000; accepted 19 February 2001

Alternative *b/y* pathway: N-terminus as nucleophile



Lower in energy than oxazolone!

Oxazolone fragment structure identified by spectroscopy

*Journal of
The American Society
for
Mass
Spectrometry*

ASMS

February 2009
Volume 20
Number 2

The diagram illustrates the CID fragmentation of the protonated tri-alanine ion ($AAAH^+$) into the b_2 fragment. Two possible structures are shown: diketopiperazine (orange) and oxazolone (green). Below the structures is an IR spectrum plot showing the characteristic absorption bands for both structures, with the x-axis labeled in cm^{-1} (800, 1200, 1600, 2000).

IR spectrum

800 1200 1600 2000 cm^{-1}

The b_2 fragment ion from protonated tri-alanine has an oxazolone, and not a diketopiperazine, structure, see page 334.

ELSEVIER ISSN 1044-0305

b_2 from AAA

Oomens, Young, Molesworth, van Stipdonk, *JASMS* **2009**, 20, 334

b_2 from AGG

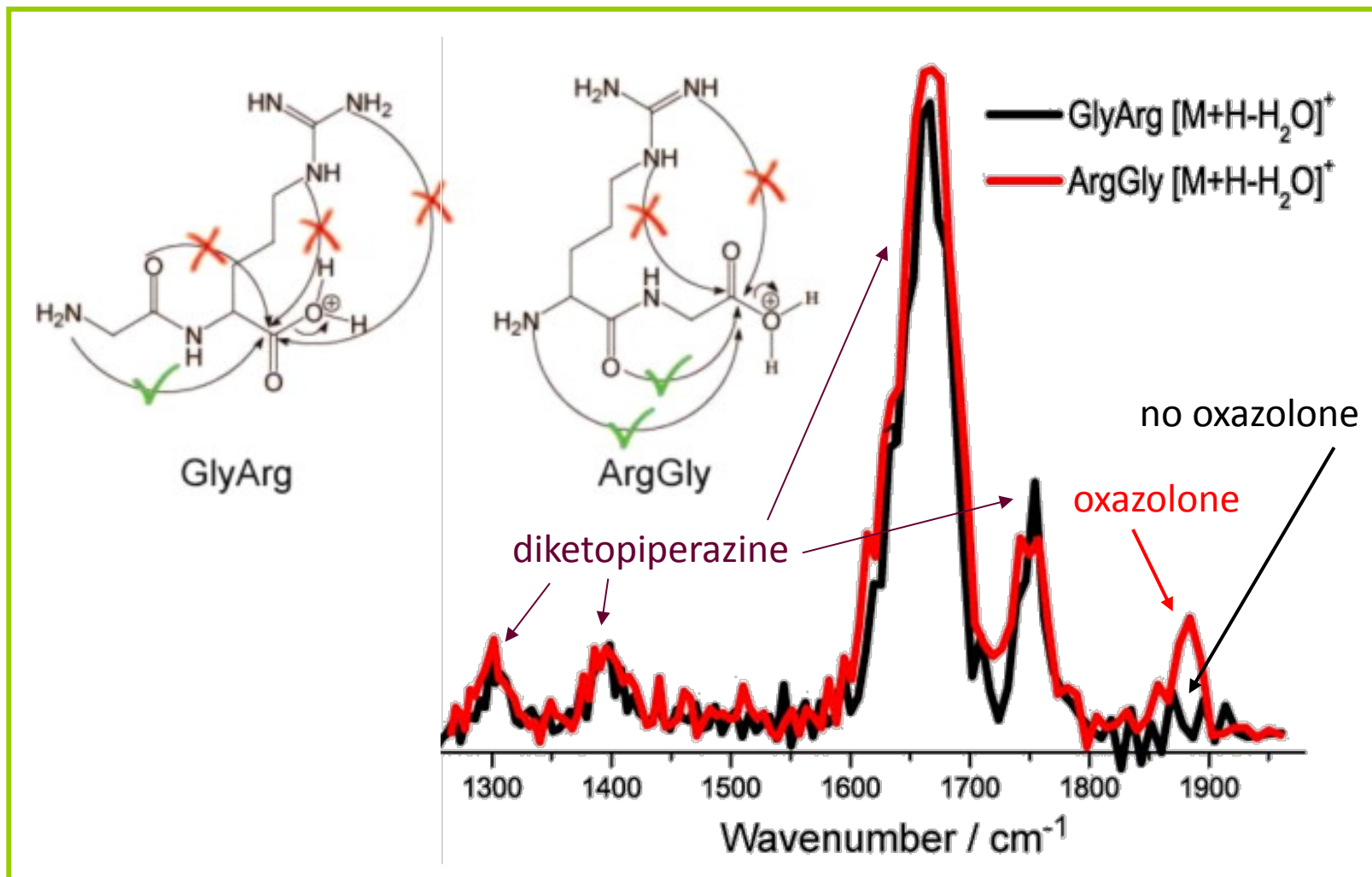
Yoon, Chamot-Rooke, Perkins, Hilderbrand, Poutsma, Wysocki *JACS*, **2009**, 20, 334

b_2 from GGG

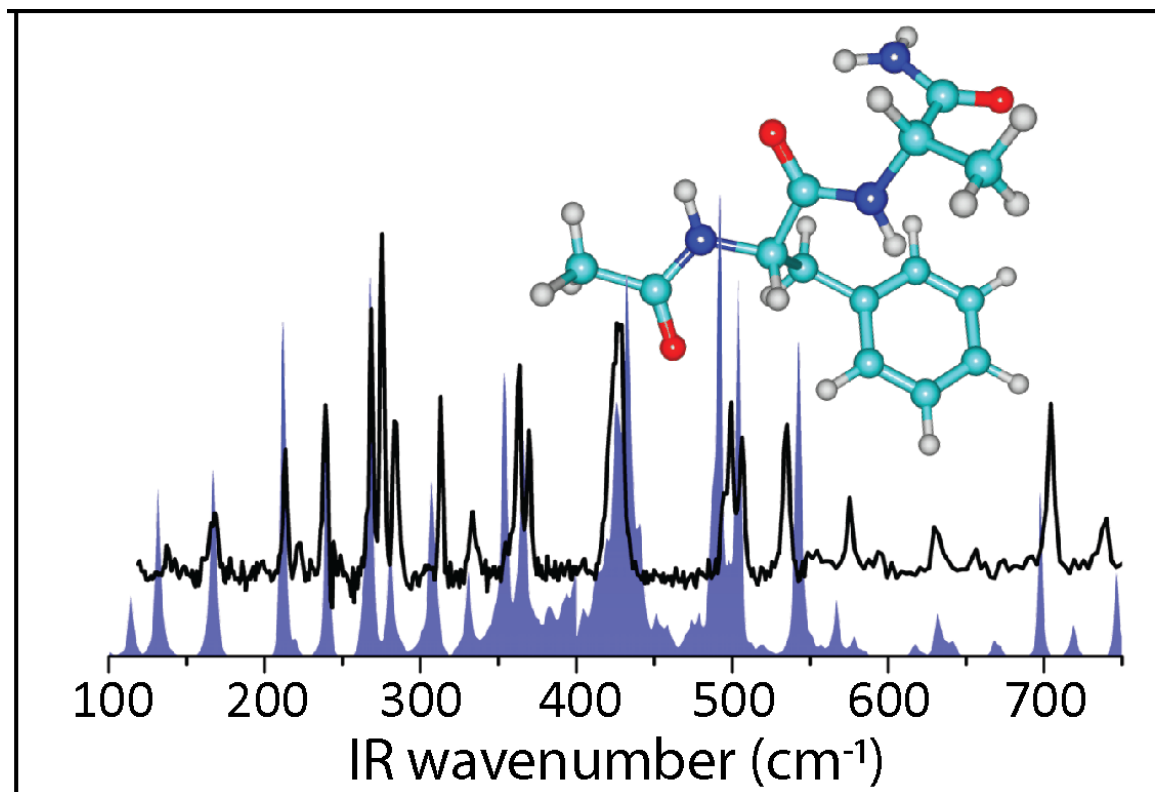
Chen, Steill, Oomens, Polfer, *JACS*, **2009**, 191, 18272

N-terminus as nucleophile: Arg

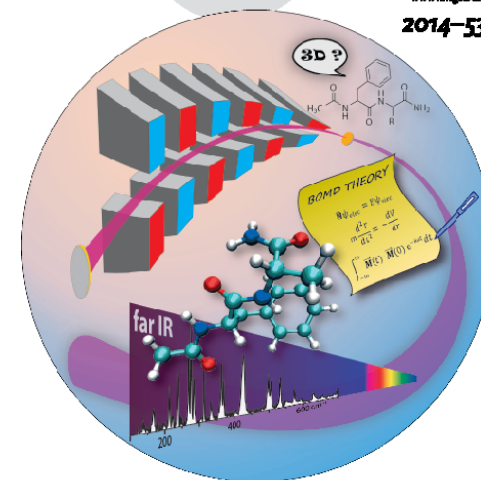
H₂O-loss from protonated GlyArg and ArgGly



Spectroscopy in the THz range



A Journal of the Gesellschaft Deutscher Chemiker
Angewandte Chemie
International Edition
www.angewandte.org
2014–53/14



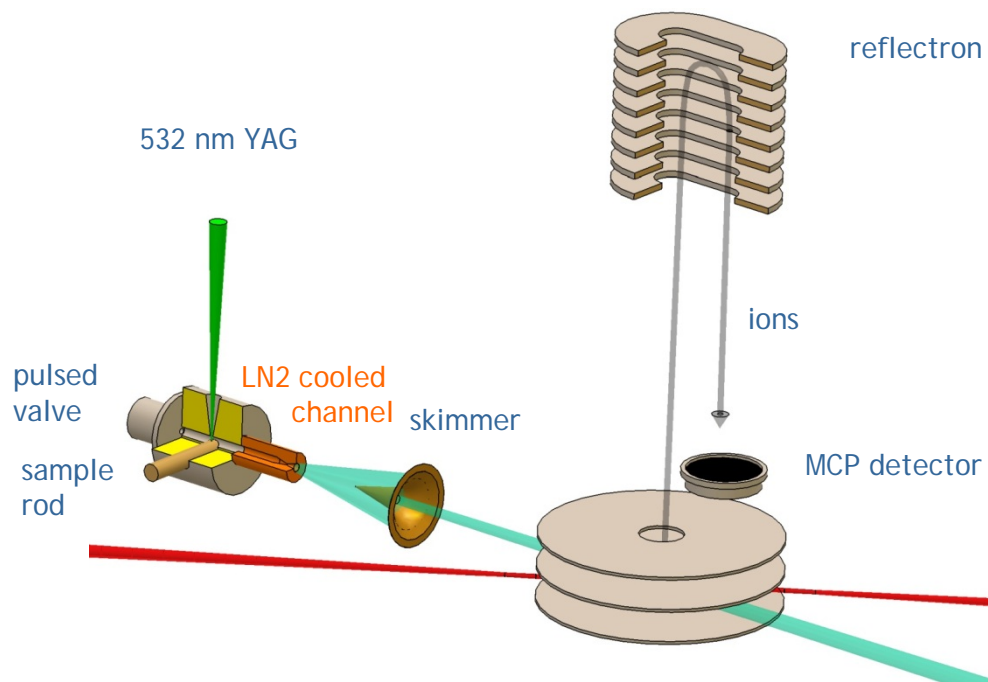
Soft vibrational modes ...

... are typically delocalized over the entire molecule. A far-infrared spectrum is therefore expected to contain detailed information on the global conformational structure of peptides. In their Communication, on page 3563 ff, M.-F. Gaigrot, A. M. Fijis, and coworkers show that conformation-selective far-IR spectroscopic experiments combined with Born-Oppenheimer molecular dynamics (BOMD) simulations provide an alternative approach to decipher this information.

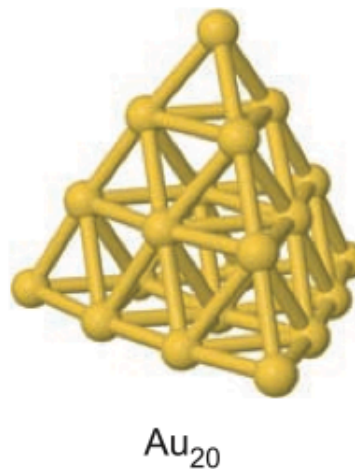
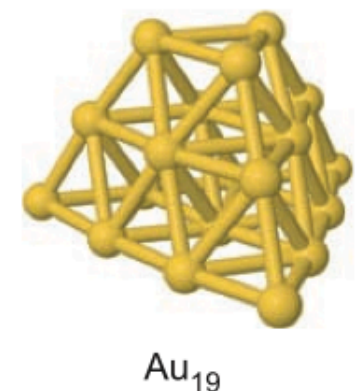
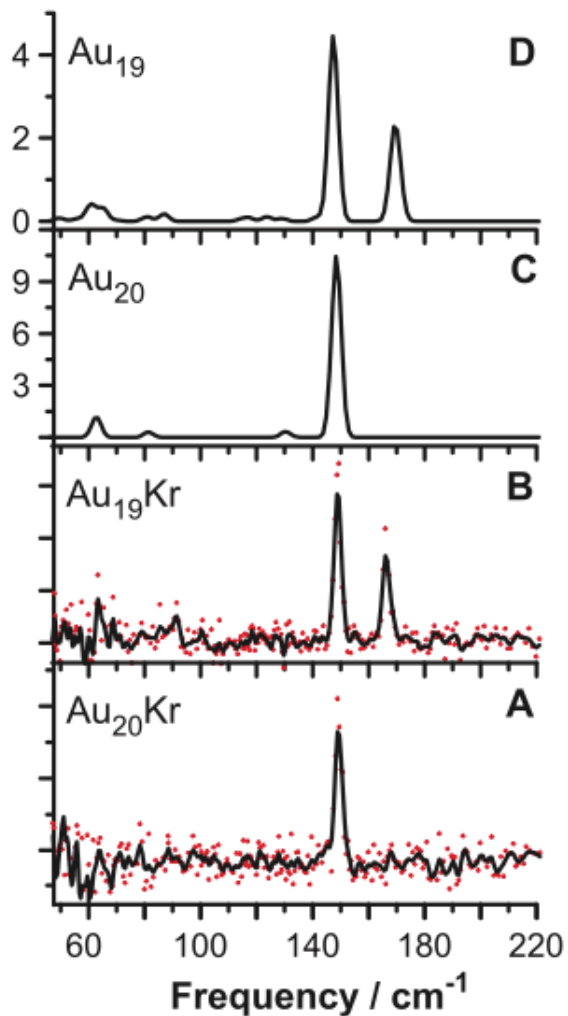
WILEY-VCH

Production of clusters

- Smalley-type cluster source
- Laser vaporization of metal rod in presence of He
- Clusters cooled to $\sim 100\text{K}$
- *Optional: reaction gas added in reaction channel (prior to expansion)*
- Interaction with laser(s)
- Mass spectrometric detection



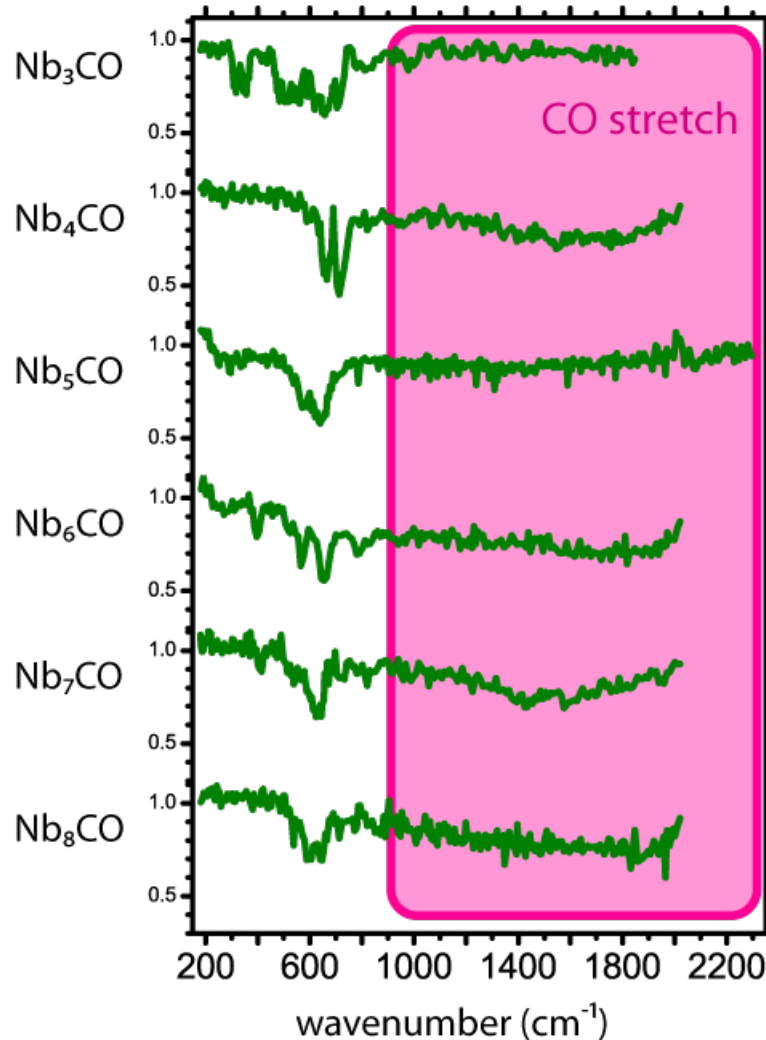
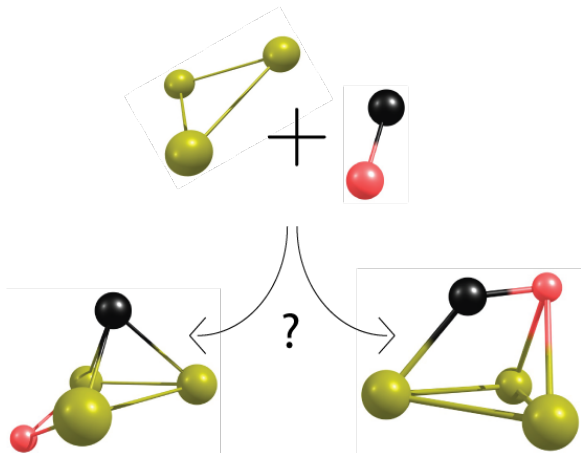
Catalysis: Structure determination of metal clusters



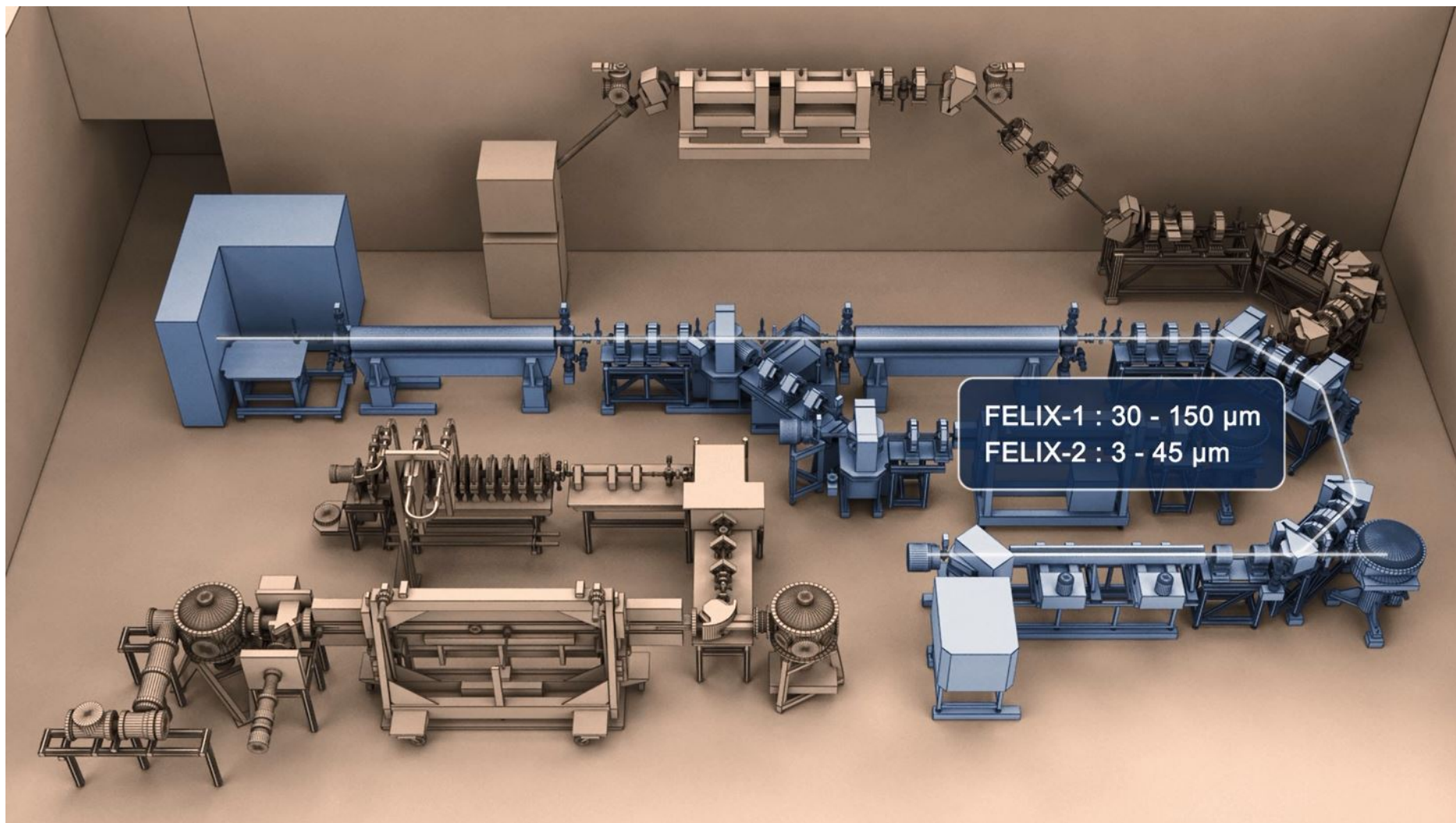
Gruene, *Science* **321**, 674 (2008).

Catalysis: Molecular vs dissociative adsorption

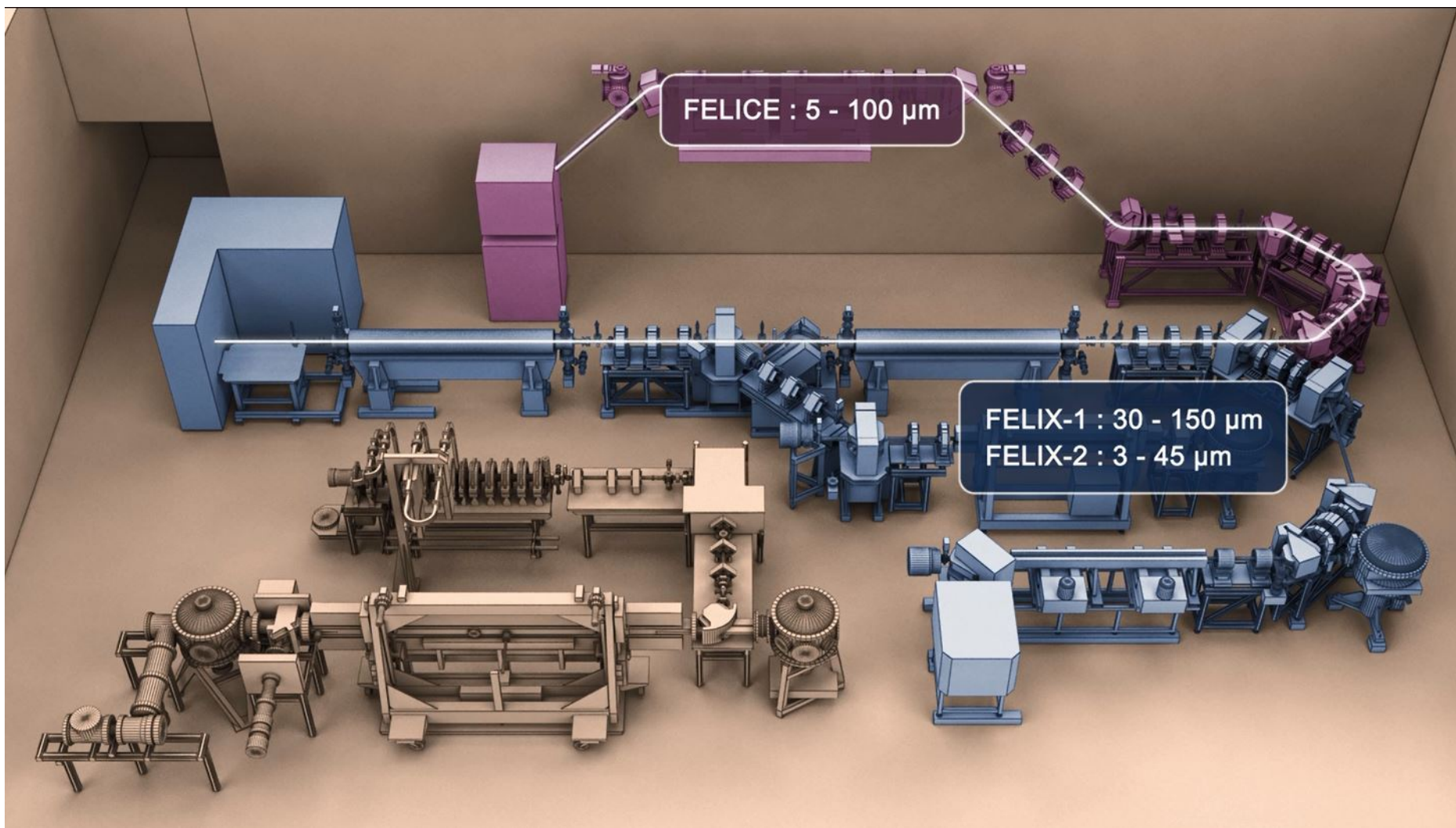
CO adsorption on metal clusters



The FELIX Laboratory



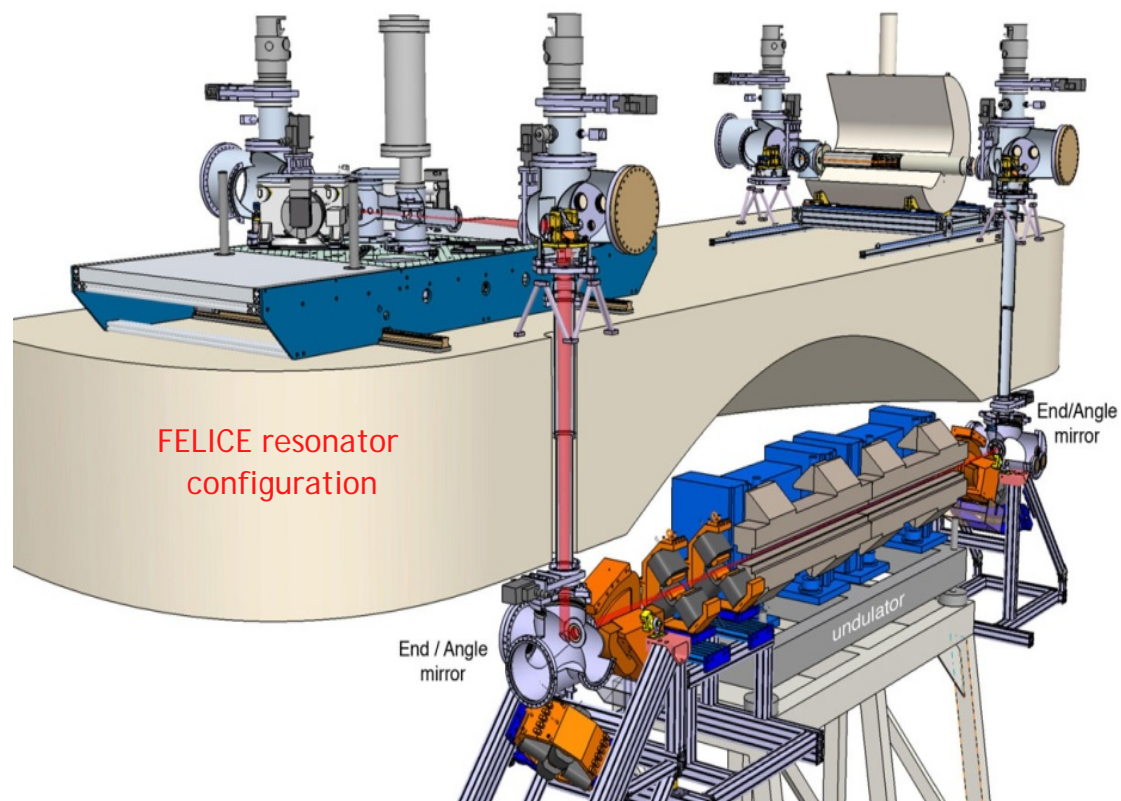
The FELIX Laboratory



The FELICE beam line

molecular beam experiment

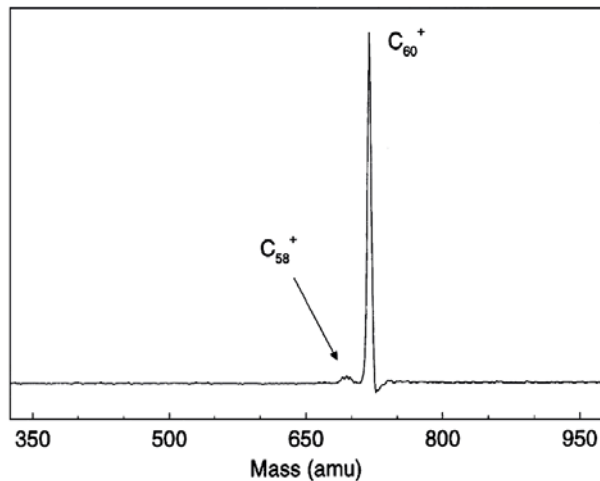
FTICR-MS experiment



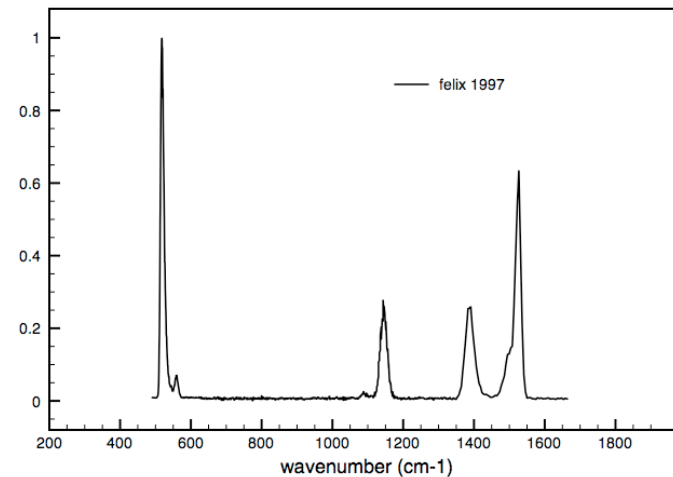
FELIX vs FELICE

mass spectra

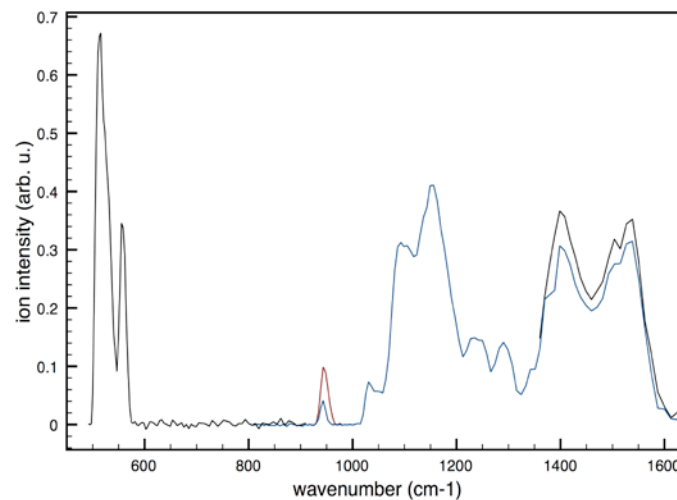
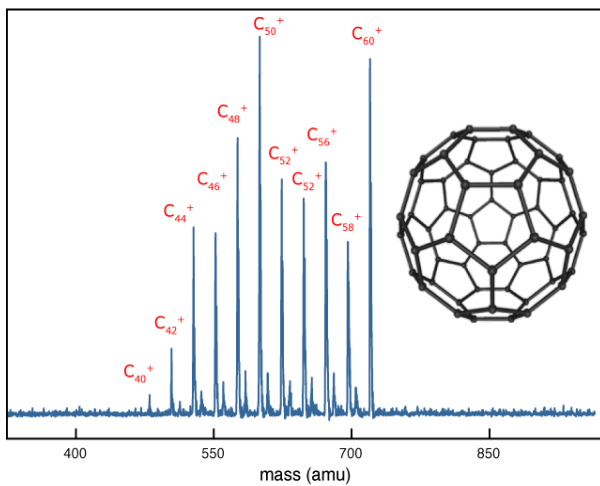
FELIX



IR spectra



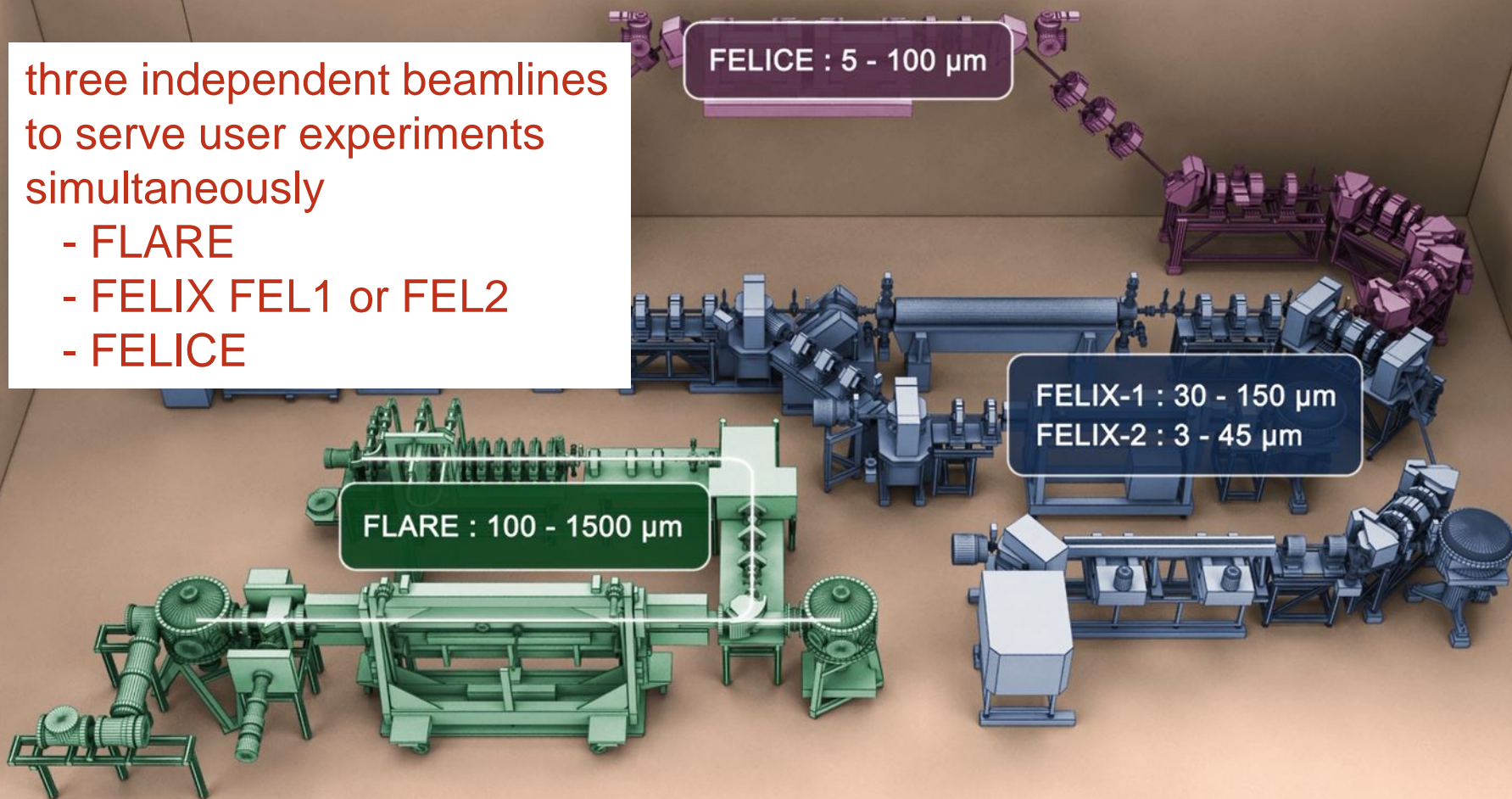
FELICE



The FELIX Laboratory

three independent beamlines
to serve user experiments
simultaneously

- FLARE
- FELIX FEL1 or FEL2
- FELICE



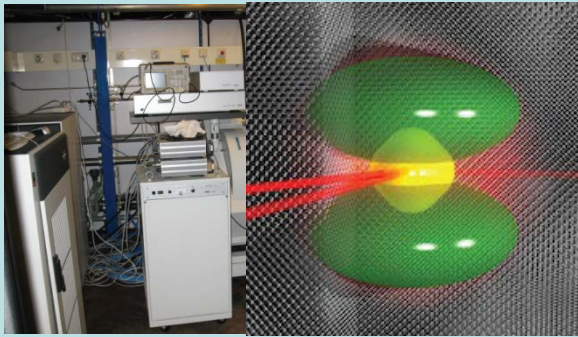
FELIX facility @ Nijmegen: User Laboratories

User laboratory 1 – FLARE & FELIX

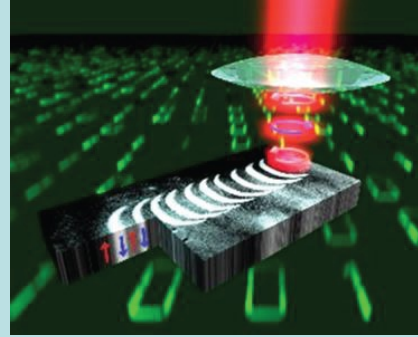
He-droplet machine
Havenith (Bochum)



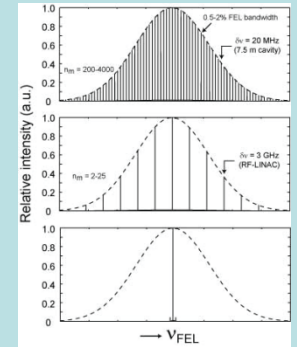
Dilution Refrigerator
EPSRC, Aeppli, Murdin



Ultrafast laser system
Kimel & Rasing (RU)



FLARE Diagnostic
Station



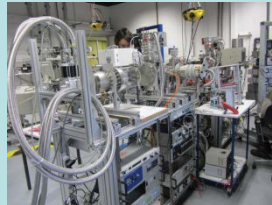
Cold 22-pole ion trap
Schlemmer (Cologne)

Molecular beam
apparatus

Paul type Ion trap

multi-purpose
station with
optical table

To be defined
(currently construction of
FLARE beam line)



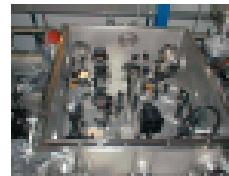
FELIX facility @ Nijmegen: User Laboratories

Ultrafast laser systems

US11



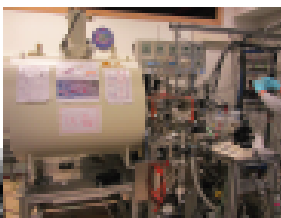
US10



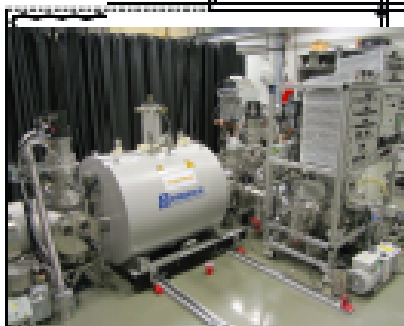
Non-linear optics laboratory

Versatile FTICR mass spectrometer

US12



FELICE 1



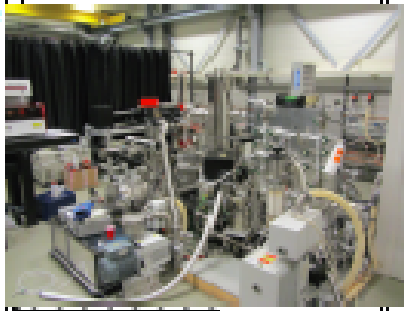
FELICE
FTICR mass spectrometer

US13

Bruker ion trap

Cluster setup

FELICE 2



FELICE
cluster apparatus

US14

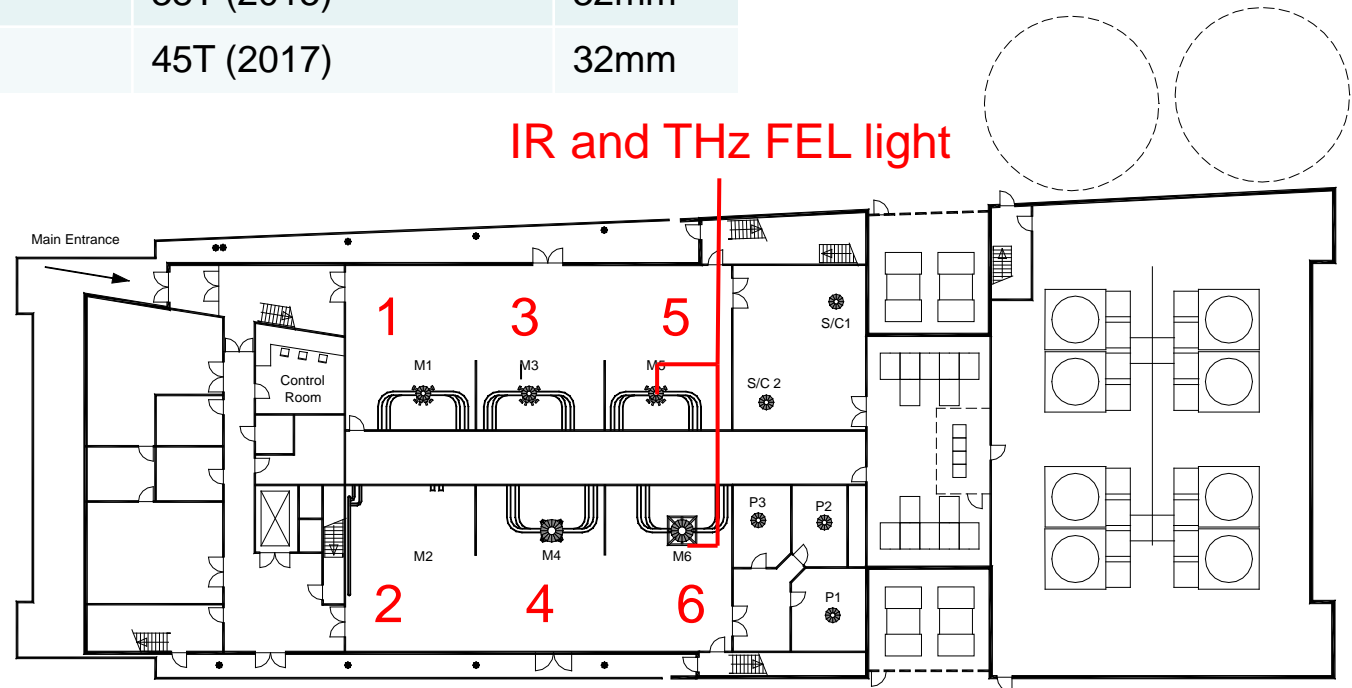
FELIX diagnostic station

User laboratory 2 -
FELIX & FELICE

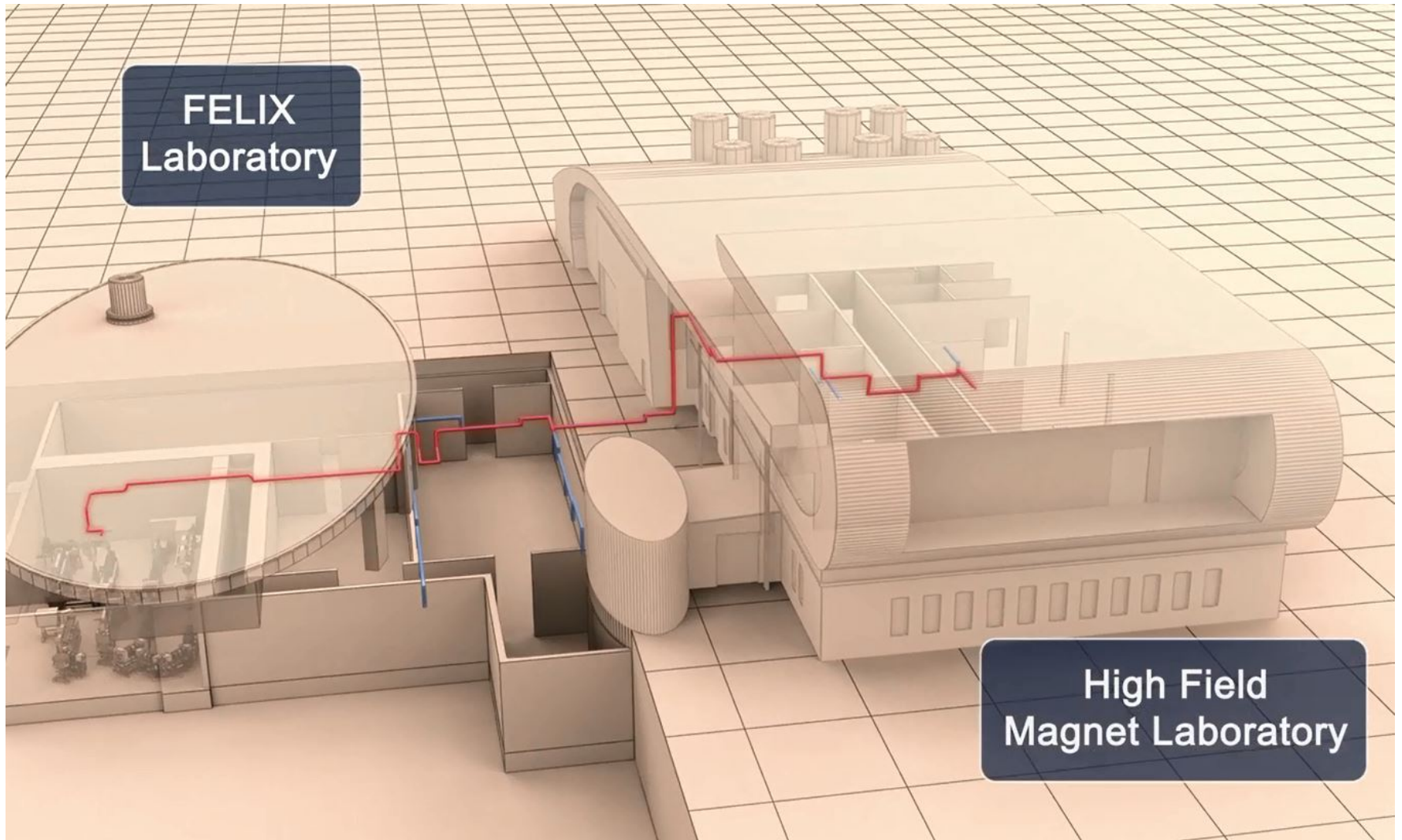
Our neighbour: HFML



Site	Magnet	Planned	Bore
1	32T (Optics above)		50mm
2	38T		32mm
3	33T (FIR above)	38T (2015)	32mm
4	30T (hybrid, 10MW)		50mm
5	33T	38T (2015)	32mm
6		45T (2017)	32mm



Combination of THz radiation and Magnetic Field



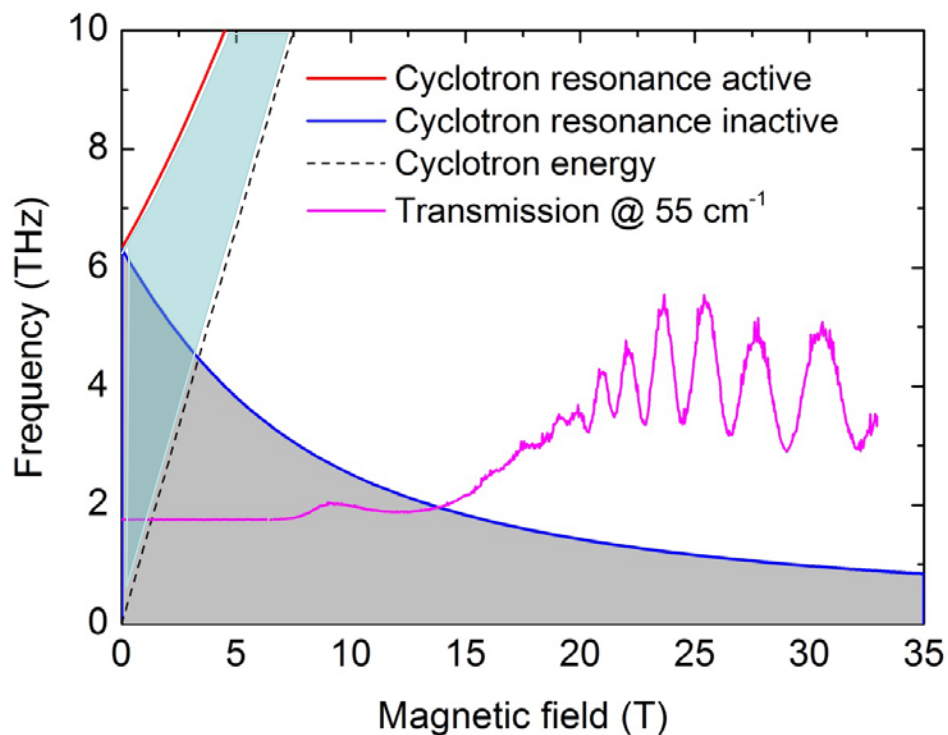
Magneto-plasma oscillations: n-type InSb

Te-doped n-InSb

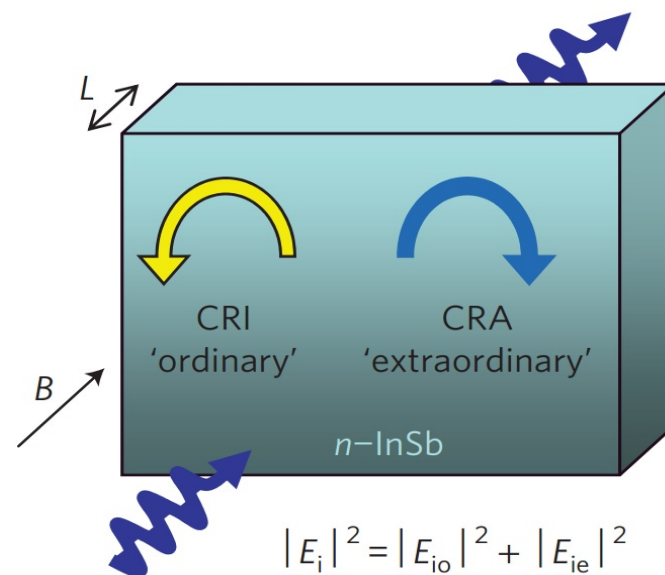
$$\omega_p = 6.33 \text{ THz}$$

$$m_{\text{eff}} = 0.021 m_0$$

$$n = 1.66 \times 10^{17} \text{ cm}^{-3}$$

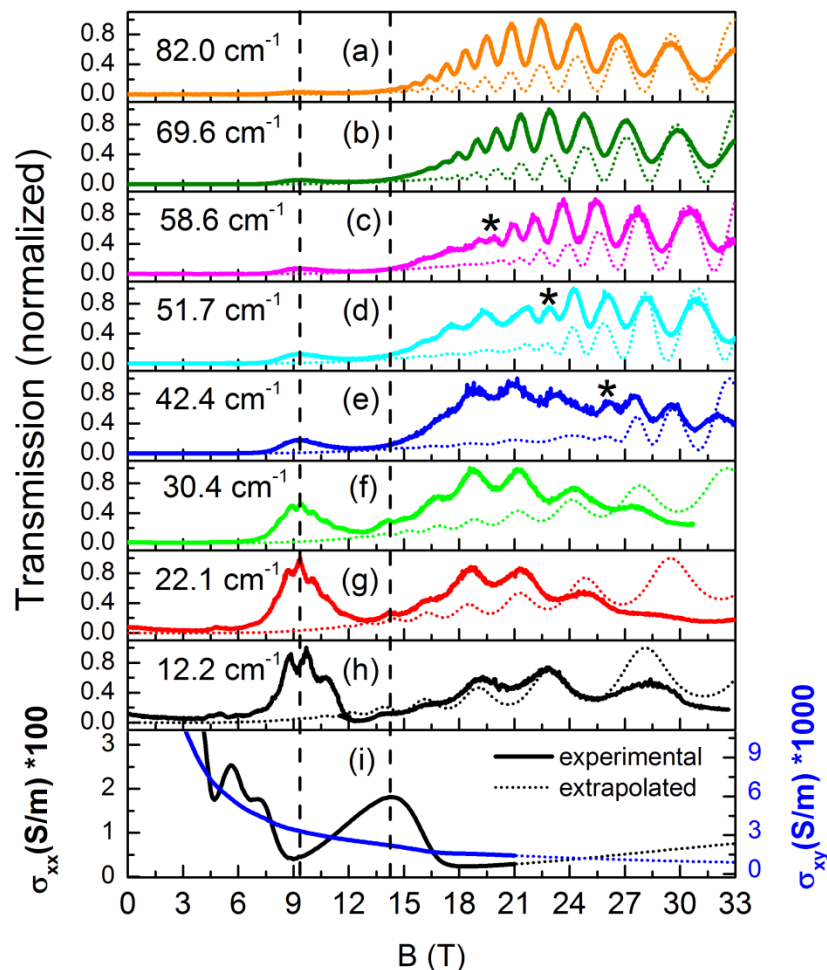


$$\frac{1}{4\pi} \left(\sqrt{\omega_c^2 + 4\omega_p^2} \pm \omega_c \right)$$



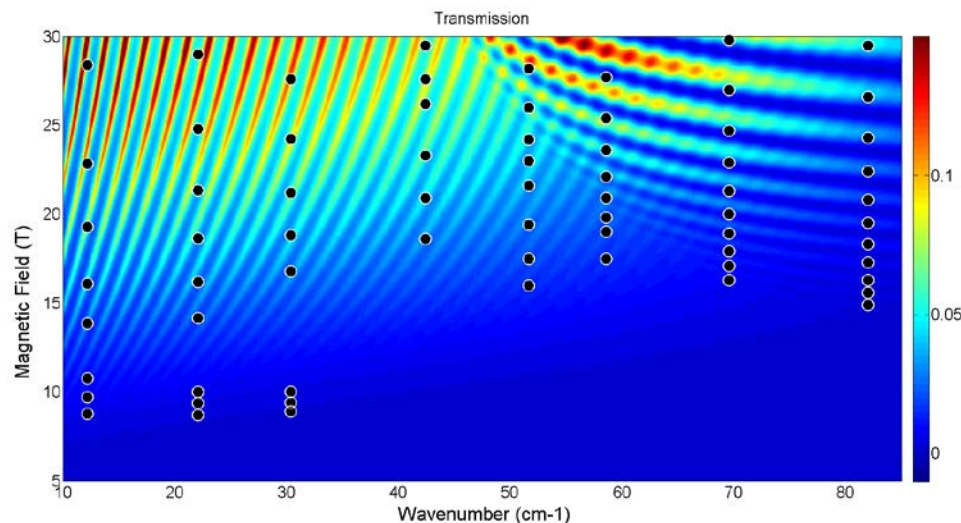
Magneto-plasma oscillations: n-type InSb

Experiment



Calculations

$$\tilde{n}_{\pm}^2 = \tilde{\epsilon}_{xx} \pm i\tilde{\epsilon}_{xy} = \kappa - \frac{\omega_p^2}{\omega(\omega \pm \omega_c + i\nu)} + \tilde{\epsilon}_{ph}$$



Thank you for your attention